Institut für Materialchemie
Institute of Materials Chemistry

DIPLOMARBEIT

Photocatalytic generation of solar fuels and simultaneous oxidation of microplastics

Ausgeführt am Institut für
Materialchemie
der Technischen Universität Wien

unter der Anleitung von
Ass. Prof. Dr.rer.nat. Alexey Cherevan
und
Univ. Prof. Mag.rer.nat. Dr.rer.nat. Dominik Eder

durch

Madeline Weisweiller, Bsc.

Wien, _____ _____

Madeline Weisweiller

Institut für Materialchemie
Institute of Materials Chemistry

MASTER THESIS

Photocatalytic generation of solar fuels and simultaneous oxidation of microplastics

Conducted at

Group of Molecular and Materials Chemistry, Institute of Materials Chemistry, Department of Technical Chemistry, Vienna University of Technology

Supervised by

Ass. Prof. Dr.rer.nat. Alexey Cherevan
Univ. Prof. Mag.rer.nat. Dr.rer.nat. Dominik Eder

By

Madeline Weisweiller, Bsc.

Acknowledgement

First and foremost, I would like to express my deepest gratitude to my supervisor, Dr. Alexey Cherevan, who has supported me every step of the way. It was an absolute pleasure working on this project with him, as every meeting concluded in good input and very insightful views. He has inspired me since the first day that I met him, with his kind heart and love for detail and chemistry. I consider him a true mentor, as I have learned so much from him and I am looking forward in continuing to do so.

Secondly, I would like to thank Professor Dominik Eder, who also often provided a valuable perspective to the project. The group he has established made me excited in participating in research and has impressed me in every possible aspect.
I would like to thank all members of the Eder group from the bottom of my heart. I have enjoyed every minute with them, as I not only consider each member a fantastic scientist, but amazing human beings, that will forever have a special place in my heart. I look forward to every new memory with you guys!
Special thanks go to Markus Hofer, whose creative mind always attempted to provide solutions to my difficulties concerning the project, Jakob Blaschke, for his efforts regarding the GC, and Dr. Doğukan Apaydin, who has often given valuable knowledge to the project and who I also consider my mentor.

Moreover, I would like to thank my friends, especially the members of “Team 4 Gewinnt”, Barbara Wagner and Nicole Müller, who often shared my discombobulation – making the world alright again. Additional gratitude goes to Nadine Haselmair, a dear friend from childhood, who always supported me on my path in becoming a scientist and kindly threatened to either hit me or drag me to university whenever I thought of giving up. And last, but not least Njomza Isufaj, with whom the friendship started on my very first day in the group and continues to flourish during coffee breaks and the exchange of voice messages. I love you all dearly!

Finally, I would like to thank my family who has been there for me throughout my studies. My Dad, who always remembered my exam dates and wished me luck. My Mum, who always listened to me complain, and my brother, who barely was effected by my mood swings since I moved out, but rather happily took over my bedroom as his east wing.
I want to conclude with my gratitude towards my fiancé, Eric Schinogl. He has been a part of my academic journey from day one, first as a friend and then as my partner for life. Although many stressful phases and long nights were included, he never left my side and will forever have my heart.

Kurzfassung

Eine voherrschende Problematik des 21. Jahrhunderts, ist die Anwendung von fossilen Brennstoffen, im Bereich von Transport und Energie, aber auch als Ausgangsmaterial vieler wichtiger Chemikalien. Zusätzlich werden diese auch in der Produktion zahlreicher allgegenwärtiger Kunststoffe, wie zum Beispiel Polypropylen (PP), Polyethylenterephthalat (PET) oder (low density) Polyethylen ((LD)PE), implementiert. Die Entsorgung dieser ist zusätzlich eine Herausforderung. Der Großteil landet auf Mülldeponien, wo durch langsamen Abbau Mikroplastik ensteht. Als Mikroplastik werden maximal 5 mm große Partikel bezeichnet. Deren Auswirkungen auf die Umwelt und Gesundheit sind noch nicht vollständig untersucht. Neuerdings, wurde das Interesse auf das Konzept von „*Photoreforming*“ gelenkt. Dieses beinhaltet die simultane Produktion von Solarbrennstoffen, wie H_2 und CH_4, und das Aufwerten von Kunststoffen zu industriell bedeutsame chemischen Verbindungen.

Im Zuge dieser Arbeit, wurden die Prinzipien des „*Photoreforming*“ untersucht, mittels Ermittlung des Einflusses von Temperatur (Raumtemperatur (RT) vs. 70°), Substrat (PET, PP und LDPE), Beleuchtungsquelle (UV Lampe vs. Xe Lampe), Anwendung eines Kokatalysators (TiO_2 mit oder ohne Pt) und atmosphärische Bedingungen (inert vs. Normalbedingungen). evaluiert. Im Bezug auf Atmosphäre, wurden die Experimente entweder mit He, unter inerten Bedingungen, durchgeführt, für die anschließende Analyse von gasförmigen Produkten, oder Luft (compressed air (CA)) beigesetzt, um die Oxidation des Substrats zu fördern und die gebildeten Produkte in Lösung zu ermitteln. Des Weiteren wurden Experimente, zur Evaluierung der zukünftigen Anwendbarkeit in der Industrie, in einem größeren Maßstab durchgeführt.

Aus den Ergebnissen lässt sich schließen, dass alle untersuchten Mikroplastikquellen erfolgreich photokatalytisch zu hochwertigen Produkten prozessiert wurden. Weiters, konnte eine Methode erfolgreich etabliert und eine Vergößerung des Maßstabs durchgeführt werden. Sowohl eine erhöhte Temperatur, als auch die Anwesenheit von Pt haben die Bildung von H_2 (1,42 µmol/h) und CH_4 (0,09 µmol/h) stark begünstigt. Es konnte keine Förderung des Substratabbaus durch Hinzugabe von Luft festgestellt werden. Daraus lässt sich schließen, dass der vorliegende Oxidationsmechanismus hauptäschlich über direketen Lochtransfer stattfindet. Im Zuge der Analyse der flüssigen Phase, konnten Oxalsäure (OA), Essigsäure (AA) und Ethylengylkol (EG) als Produkte festgestellt werden. Hiebrei konnten die höchsten Umsätze für AA (15,8%) und EG (9,5%) erzielt werden. Jedoch konnte bis jetzt keine direkte Korrelation der Ergebnisse zu den angewendeten Paramtern identifiziert werden.

Abstract

A predominant issue of the 21st century is the employment of fossil fuels, for transport, energy and as feedstock for many important chemicals, which all lead to their to detrimental impact on the environment. In addition, they are utilized for the production of everyday plastics, such as polypropylene (PP), polyethyleneterephthalate (PET) and (low density) polyethylene ((LD)PE). Their abatement is a further concern, as a majority is deposited onto landfills, slowly degrading to microplastics, which are particles constituting less than 5 mm in size. Their precarious impact on both the environment and health are yet to be fully established. In recent years, *photoreforming*, which describes the simultaneous generation of solar fuels, such as H_2 and CH_4, and the upcycling of plastics to high-value-added chemicals, has gained a lot of interest.

In this work, the concepts of photoreforming were studied by investigating the effect of temperature, substrate, irradiation source, presence of a co-catalyst on TiO_2, and atmospheric conditions on the process. Hereby, the focus was set on the comparison between room temperature (RT) and 70°C, UV irradiation and a broad-band Xe lamp, neat P25-TiO_2 and the one with Pt as co-catalyst examining PET, PP and LDPE as substrate. The reaction solution was either purged with He, for inert conditions and investigation of the gaseous products, or compressed air (CA), to expedite oxidation of the investigated substrate and analysis of products in the liquid phase. Furthermore, the feasibility for future industrial application was also of interest, thus experiments in an upscaled manner were additionally conducted.

My results demonstrate that all studied microplastic sources could be successfully processed by means of photocatalysis, resulting in a mixture of high-value products. In addition, the established methodology has provided reproducible results and a scaleup was achieved. Both exalted temperature and the employment of Pt resulted in the highest quantities of H_2 (1,42 µmol/h) and CH_4 (0,09 µmol/h). Moreover, no beneficial impact of CA on the degradation of the substrates could be concluded, which shows that direct hole transfer is the predominant oxidation pathway for the investigated samples. When analysing liquid-phase products, oxalic acid (OA), acetic acid (AA) and ethylene glycol (EG) were found, with the highest conversion rates presented by AA (15,8%) and EG (9,5%). However, no direct correlation to the applied parameters of the respective samples could for now be established.

List of abbreviations and symbols

AA	*acetic acid*
CA	*compressed air*
CB	*conduction band*
CH_4	*methane*
CO	*carbon monoxide*
CO_2	*carbon dioxide*
e^-	*electron*
E_g	*bandgap*
EG	*ethylene glycol*
FA	*formic acid*
GC	*gas chromatography*
h^+	*hole*
H^+	*proton*
H_2	*hydrogen*
He	*helium*
HER	*hydrogen evolution reaction*
HOMO	*highest occupied molecular orbital*
HPLC	*high pressure liquid chromatography*
hv	*energy of electromagnetic wave (light)*
IR	*infrared*
(LD)PE	*(low density) polyethylene*
LUMO	*lowest unoccupied molecular orbital*
NaOH	*sodium hydroxide*
OA	*oxalic acid*
OER	*oxygen evolution reaction*
P25	*mixture comprised of both rutile and anatase TiO_2*
PET	*polyethylene terephthalate*
PP	*polypropylene*
Pt	*platinum*
ROS	*reactive oxygen species*
RT	*room temperature*
SD	*standard deviation*
TiO_2	*titania*
UV	*ultraviolet*
VB	*valence band*
Xe	*xenon*

Table of content

1. Introduction

1.1 Plastic waste – the debris of a synthetic civilisation

Plastics are an ubiquitous material deeply implemented in everyday life. It has been established that the global annual consumption of plastics has grown severely in the last decades. This is due to a number of advantageous properties, including but not limited to, their light weight, inexpensive fabrication and low density.[1,2] Consequently, this type of material is employed in numerous applications, such as packaging, building and construction and medical materials.[1,3] Among the most commonly used plastics are polyolefins such as ***(a)*** polypropylene (PP), ***(b)*** polyethylene (PE), ***(c)*** polystyrene (PS), polyesters like ***(d)*** polyethylene terephthalate (PET) and ***(e)*** polylactic acid (PLA), but also halogen containing compounds, for example polyvinylchloride ***(f)*** (PVC) and ***(g)*** polytetrafluoroethylene (PTFE).[4] The structures of these aforementioned common polymers are depicted in ***Figure 1***.

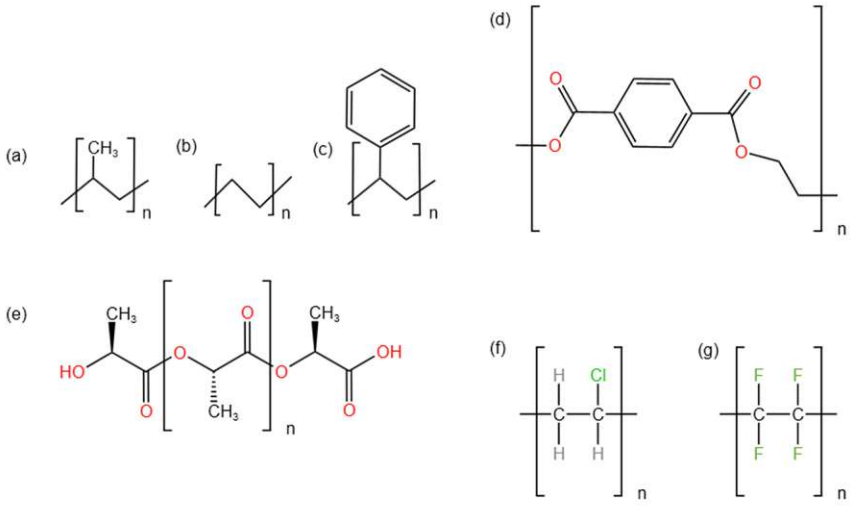

Figure 1*: Structures of some of the most common commercial polymers – (a) PP, (b) PE, (c) PS, (d) PET, (e) PLA (S - configuration), (f) PVC and (g) PTFE.*

In a span of just 65 years, from 1950 to the mid-2010s, around 6 billion tons of plastic waste has been produced. This is a major issue, as only a mere 9% has been recycled, a little over 10% incinerated and the vast majority, around 80%, has ended up in landfills or has been deposited into the environment.[5] These released waste products persevere for decades or even centuries before full natural degradation occurs.[6] The decomposition is further prolonged due to a great number of additives in commercially available plastic products, for instance stabilizers, antioxidants or flame retardants.[7] Furthermore, the polymers form debris of micro- and nano plastics when degradation does take place. This not only affects animals, crops and humans, but also marine life. It has been reported that single-use plastic products constitute 50% of the waste scattered on European beaches and oceans. As a result, a very large number of marine

organisms, for example turtles or whales, die due to ingestion of the pollutant or entanglement in plastic waste.[3,4] Microplastics, with a particle size of 5 mm or less, is especially a concern due to the contamination of the environment and subsequent accumulation in food and water. This type of debris can exhibit a variation of properties in respect to size, shape, density and ramification on living organisms, depending on polymer type and source. Moreover, in addition to soil and aquatic environments, microplastics have also been found in human faeces and placenta.[8]

It is also believed that microplastics can incorporate noxious waste substances, such as heavy metals. This poses a further health risk.[9] Notably, the adverse effects of heavy metals on organisms are a heavily discussed matter. Depending on metal and metal-containing compounds and the duration of exposition and concentration, heavy metals are known for their carcinogenicity and neurotoxicity for example.[10] In a work carried out by *Ashton et al.* heavy metals, such as iron, manganese and lead, were successfully adsorbed onto PE pellets from seawater. Further, it appears that adsorption ability of the investigated microplastics increased with age, surface area, porosity and polarity.[11] This underlines the necessity in obtaining a possibility for the extraction or removal of plastic pollutants, of any kind, from the environment.

1.2 The global energy crisis

Fossil fuels constitute the main energy source to this day. However, this is not without consequence. Some of the most concerning repercussions that we are confronted with in the 21st century are air pollution and global warming.[12] Emissions associated with fossil fuels, for example, have contributed to a rise in pulmonary and cardiovascular conditions respectively, and thus an increase in mortality rate.[13] In addition, global warming has adverse effects on the environment and the human population. Worryingly, when temperatures rise, environmental disasters like tsunamis, droughts, heavy rains, and earthquakes as well as disease outbreaks will occur more frequently. Consequently, food supply and habitat are endangered.[14] As a response to this issue, efforts have been made to prevent further temperature elevation. In 2015, the Paris agreement was enacted. Herein, the limitation of temperature increase to 1.5 °C in respect to the preindustrial era, was stated as a goal. In order to achieve this, it appears that an alternative to fossil fuels is required imminently.[15] More recently, the European Green Deal was presented in December 2019. Here, complete climate neutrality accomplished by 2050 became the new target for Europe.[16] Though the intentions of both agreements are a step in the right direction, it is yet a major challenge to renounce fossil fuels completely. Currently, they are deeply embedded in daily life, acting as a source for crucial chemicals or, for example, as gas for heating or transportation. Moreover, the production of plastics greatly relies on fossil fuels. Overall, 99% of feedstock utilised for the synthesis of plastics is comprised of hydrocarbon deposits.[17]

To overcome this issue, there is an exalted enthusiasm in the research for renewable energy sources as substitutes. As of now solar and wind power technologies have proven to be outstanding alternatives as well as being inexpensive.[18] Furthermore, the synthesis of green hydrogen (H_2), a novel renewable energy source, has rapidly gained attention. H_2 as such is an essential precursor for the industrial synthesis of numerous exceedingly valuable chemicals, such as methanol, but also ammonia, which makes meeting the great demand for food, with the growing numbers in population, feasible. A major drawback are the current methods for obtaining H_2. Presently, roughly 99% is produced from fossil fuels, such as petroleum or coal, and a mere 0.7% from water electrolysis. This further accentuates the urgency in acquiring a beneficial synthesis approach for green H_2, as it would provide a novel source of energy with zero emissions and subsequently avert further detrimental impacts on the ecology.[13,18,19]

Many efforts have been made in the last decades in order to accomplish this milestone. Due to this, the scientific community has become very dedicated in the production of green H_2 by water splitting with the aid of photocatalysis.

1.3 Heterogeneous photocatalysis

In principle, photocatalysis is based on a catalyst, which modifies the rate of a chemical reaction upon illumination with light. This research field can be subdivided into two categories. On one hand there is the class of *homogeneous photocatalysis*, where both the photocatalyst and the respective reactant are present in the same phase, which is most often liquid. In contrast, the second class is *heterogeneous photocatalysis*. This describes a *semiconductor*, as the photocatalyst, interacting with a reactant in a liquid phase.[20]

A semiconductor is a solid-state material, which possesses a bandgap (E_g), as is illustrated in ***Figure 2***. The bandgap is defined as the difference in energy between the highest occupied molecular orbital (HOMO) and lowest occupied molecular orbital (LUMO). Herein, the HOMO is equivalent to the valence band (VB) and the LUMO to the conduction band (CB). The presence of the bandgap is key for every photocatalytic process, as it enables the production of electron-hole pairs, which are the charge carriers able to run and catalyse the reduction and oxidation process. Consequently, neither *insulators* nor *conductors* would be applicable for this, as the bandgap value of the former is larger than that of a semiconductor, whilst the latter does not own a bandgap. This is also displayed in ***Figure 2***.[20]

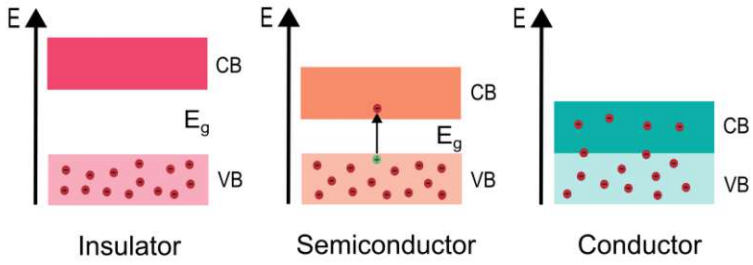

Figure 2: *This image demonstrates the band positions of an insulator (left), a semiconductor (middle) and a conductor (right); red dots = negatively charged electrons, green dot = positively charged hole.*

Additionally, the utilisation of semiconductors as photocatalysts is beneficial, as ambient conditions are sufficient for the conduction of photoexcited charges, thus no elevated temperatures or pressures are necessary. The photons of light are typically absorbed by the bulk of the semiconductor, leading to the excitation of the VB electrons (e^-) to the CB and, concurrently, to the formation of a positively charged hole (h^+) in the VB. In order for this process to take place, it is essential that the energy of these absorbed photons has an equal or greater energy value than the bandgap of the semiconductor. The generation of the electron-hole-pair, the exciton, is crucial for every photocatalytic process, as the e^- in the CB is then capable of reducing an acceptor molecule and the h^+ in the VB is able of oxidising adsorbed species, thus the donor molecule. Therefore, oxidation and reduction reaction both occur simultaneously during photocatalysis and

on the surface of the photocatalyst. It is essential that both e^- and h^+ are rapidly driven to or trapped on the surface of the semiconductor to thus avert recombination of these attractive charges and guarantee successful redox reaction.[20–22]

The focus of this work was set on the application of heterogeneous photocatalysis, as is described in the following chapters. This class of photocatalysts has proven to be feasible for numerous applications, such as water and air purification, drug delivery, selective reduction and oxidation of organic substances and water splitting.[22]

1.3.1 Water splitting

In 1972, groundbreaking research was conducted by *Fujishima and Honda* in the field of photocatalysis. They succeeded in splitting water in its respective molecules, H_2 and O_2, without the requirement of external voltage. The water photoelectrolysis was performed with platinum (Pt) and titania (TiO_2) as electrodes. Illumination of the photoelectrochemical setup resulted in an electrical current flowing through an external circuit from the TiO_2 anode to the Pt cathode. It was established that the oxidation process, also described as oxygen evolution reaction (OER), was taking place at the TiO_2 electrode. The reduction reaction, i.e. the hydrogen evolution reaction (HER), was observed at the Pt electrode. The below ***equations (1) - (3)*** demonstrate each of these half reactions and the sum of both. Moreover, a potential difference between the electrodes of at least 1.23 V is required to accomplish successful electrochemical splitting of water. As this potential is equivalent to around 1000 nm in wavelength, it appears feasible to obtain both H_2 and O_2 from water with the assistance of visible light.[23,24]

$$oxidation: \quad 2\,H_2O + 4\,h^+ \rightarrow O_2 + 4\,H^+ \qquad \textbf{(1)}$$

$$reduction: \quad 2\,H^+ + 2\,e^- \rightarrow H_2 \qquad \textbf{(2)}$$

$$reaction\ sum: \quad 2\,H_2O \rightarrow 2\,H_2 + O_2 \qquad \textbf{(3)}$$

Since this discovery, the application of TiO_2 as a photocatalyst has been extensively studied. This metal oxide has a great number of beneficial properties, such as cost efficiency, chemical stability, rather good photocatalytic activity, and hydrophilicity.[22] Due to a bandgap value greater than 3.2 eV, application in water splitting is attainable. As mentioned above, breaking water into its components requires a bandgap value of 1.23 eV, yet due to kinetic requirements a bandgap larger than 2.0 eV is crucial for successful H_2 and O_2 production. Though TiO_2 fulfils this, it is merely efficient in interacting with photons of the UV portion of solar light, as visible light absorption requires a bandgap value below 3.0 eV.[25] This especially is a drawback, as sunlight is comprised of visible light by 50% and a mere 4% of UV. An additional issue in respect to TiO_2 as

a photocatalyst, are so-called recombination processes. These entail the photoexcited e^- in the CB recombining with the positively charged h^+ in the VB, as opposite charges attract each other by nature.[21]

Overall, there are a number of parameters that are essential to consider in the synthesis of a photocatalyst and have an impact on its performance. This includes its crystallinity, as the probability of charge recombination occurring can be minimized by the presence of certain defects, surface properties, as a large surface area facilitates substrate adsorption, but also the presence of impurities and dopants.[24,25] Many efforts have been made in respect to the enhancement of photocatalytic activity. This may be achieved by adding a metal co-catalyst, often noble metals like Pt or Pd, dye sensitization or even heterojunction formation with other materials, like graphene for example.[21]

There are two polymorphs of TiO_2 which are relevant in photocatalysis – rutile and anatase. Rutile for example possesses a bandgap value of around 3.0 eV and is a direct bandgap semiconductor. In contrast, anatase is an indirect bandgap semiconductor, which has a bandgap value of around 3.2 eV. This prolongs the life of the generated charge carriers and subsequently increases the probability of a redox reaction taking place. As a result of their varying surface properties and mechanisms, in respect to exciton excitation and migration, both crystal structures display diverging photocatalytic activity. However, they are both active under UV irradiation.[26,27] As an approach to benefit from auspicious properties of both rutile and anatase, a powdered mixture, known as P25, is commercially available. The blend of these crystallites exhibits greater catalytic activity than the neat phases, due to facilitated charge separation between the two.[26,28]

Besides TiO_2, there are many other semiconductors currently of interest in this field. For example, cadmium sulfide (CdS) is often investigated, as it possesses a narrow bandgap of 2.4 eV and thus can absorb visible light.[29] Other visible light active photocatalysts for example include tungsten oxide (WO_3)[30] and graphitic carbon nitride (g-C_3N_4).[31]

Achieving the production of green H_2 through water splitting via photocatalysis has shown great potential, especially as an inexpensive substitutional energy source. A great amount of research has been made regarding modification of the present photocatalysts, to improve their performance, through dye sensitization, anion doping or loading with metal co-catalysts.[21]

1.4 Photocatalytic plastic degradation and upcycling

As mentioned in previous chapters, photocatalysis has gained a lot of attention in the past decades. As research in this topic has evolved, further applications have also been investigated. Currently, most of plastic waste is deposited in landfills or combusted. The latter not only requires high temperatures, but also causes adverse effects on the environment due to the release of noxious gaseous by-products.[4,32] The prior mentioned polymers, PE, PP, PS and PVC, further classified as additional polymers, are regarded as non-biodegradable. This is due to their backbone being comprised of C-C bonds, which prohibit hydrolytic cleavage or degradation taking place. In contrast, the structure of condensation polymers, PET for example, additionally incorporate O and/or N in their backbone. These polymers are prone to hydrolytic cleavage as a consequence of hydrophilic ester or amide linkage between the monomers, which makes their degradation or potential recycling more achievable.[7] Although recycling is desirable, given the disadvantageous properties of plastics, it is less cost-efficient, as it requires the separation of complex polymer mixtures.[32,33] Further, a subcategory, known as mechanical recycling, entails grinding and extruding of polymers. This method ensures indifferent chemical properties, yet the mechanical and structural characteristics decline with every cycle.[4]

Therefore, there is a great urgency in establishing novel plastic re- and upcycling methods, due to subsequent detrimental impacts of current disposal techniques on the environment and living organisms. The complexity of this issue has motivated the scientific community to assess the feasibility of new methods by implementing the principles of photocatalysis.

1.4.1 Photodegradation of plastics

Photodegradation describes the implementation of solar energy in the break-down of plastic waste into smaller fragments. This is regarded as a green opportunity, as this results in the production of water and carbon dioxide (CO_2), solely requiring ambient conditions.[4]

During photodegradation, so-called reactive oxygen species (ROS) assist the process. Upon light absorption, in the near UV range between 290 - 400nm, a photogenerated e^- is excited to the CB, as was stated above, shown in ***equation (4)***. Though in contrast to water splitting, O_2, rather than protons (H^+), is reduced and forms superoxide anion radicals ($O_2^{\bullet-}$), displayed in ***equation (6)***. This radical can then generate hydroxyl radicals (•OH), which are a very reactive and non-selective species. Therefore, the degradation products are often comprised of very complex mixtures. This is illustrated in ***equation (7) - (10)***. The second part of the process involves the h^+ in the VB. These migrate to the surface of the semiconductor, interacting with adsorbed species, i.e. water or organic molecules. As a result, additional •OH is produced, degrading the substrate to CO_2, water and smaller organic molecules, ***equation (5)***. The formed radicals then react with

the plastic waste to the respective degradation product, ***equation (11)***. To summarize, both h^+ (direct pathway) and ROS (indirect pathway) possess the possibility to degrade plastics, which can then further lead to autooxidation.[34] Depending on the photocatalyst and microplastic present, but also on the selected reaction conditions, one or the other pathway is more prevalent.[4] The process of plastic photodegradation is displayed in ***Figure 3a***.[4,34]

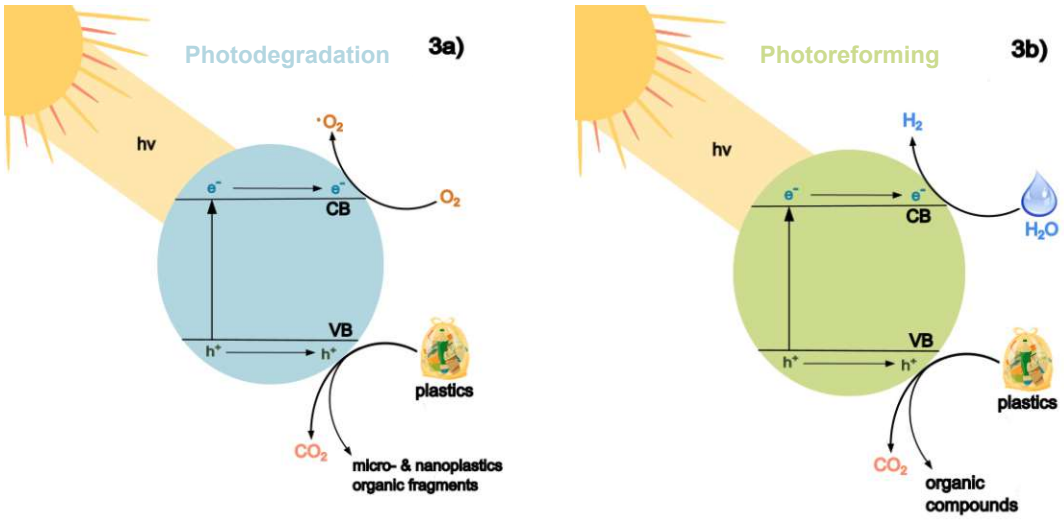

Figure 3: 3a) *Photodegradation process: top right: oxygen reduction by the e^-, resulting in ROS, bottom right: plastic waste is oxidized by the h^+ to CO_2, micro- and nanoplastics and smaller organic molecules* ***3b)*** *Photoreforming process: top right: water reduction for H_2 production, bottom right: oxidation of plastic waste into smaller organic compounds and CO_2.*

$$semiconductor + hv \rightarrow h_{VB}^{+} + e_{CB}^{-} \quad \textbf{(4)}$$

$$h_{VB}^{+} + H_2O \rightarrow \cdot OH + H^{+} \quad \textbf{(5)}$$

$$e_{CB}^{-} + O_2 \rightarrow O_2^{\cdot -} \quad \textbf{(6)}$$

$$O_2^{\cdot -} + e_{CB}^{-} + 2\,H^{+} \rightarrow H_2O_2 \quad \textbf{(7)}$$

$$H_2O_2 + hv \rightarrow 2 \cdot OH \quad \textbf{(8)}$$

$$H_2O_2 + O_2^{\cdot -} \rightarrow \cdot OH + OH^{-} + O_2 \quad \textbf{(9)}$$

$$e_{CB}^{-} + H_2O_2 \rightarrow \cdot OH + OH^{-} \quad \textbf{(10)}$$

$$O_2^{\cdot -}\ or\ \cdot OH\ or\ h_{VB}^{+} + Plastics \rightarrow Degradation\ products \quad \textbf{(11)}$$

The procedure steps of this method appear simple, which could make application on a large scale feasible.[35] First, organic solvents, such as toluene or cyclohexane, are added to the desired plastics, then the respective photocatalyst. This mixture is a precursor for a composite film, which is then implemented for the photodegradation process and contains both the photocatalyst and the plastic substrate. The reaction mixture is stirred and heated, to ensure a homogeneous dispersion. Next, the solvent is separated from the composite film via drying at elevated temperatures. This photocatalyst/plastic composite is then irradiated, thus photodegradation

takes place.[4,35] In order to subsequently ascertain the efficiency of plastic mineralization to CO_2, the weight loss of the involved substrates is determined.[4] Besides the synthesis of composite films, dissolving the photocatalyst in an aqueous solution and then covering the desired polymers with this mixture, is believed to be another opportunity for direct degradation, whilst implementing solar energy. An increase in wt.% of the photocatalyst, utilizing of a high energy light source and aerobic conditions, expedite photodegradation.[35]

The most investigated photocatalyst, for this application, has been TiO_2 as well. As aforementioned, it exhibits efficient photocatalytic activity, is non-toxic and inexpensive. In order to facilitate the absorption of visible light and the reaction between the plastic substrate and photocatalyst at the interface, and to enhance the active surface area as well, numerous concepts have been established.[35] Examples include TiO_2-P25 nanotubes or -particles, for the photodegradation of low density PE (LDPE)[36,37], but also composites, such as polypyrrole/TiO_2 for the decomposition of PE plastic bags.[38] In a great number of studies, it has been demonstrated that the degradation process of PE, for example, with the assistance of a TiO_2-based photocatalyst requires days or even weeks. Despite this rather lengthy frame, the plastic did not occur fully degraded. This has increased the motivation of this field of research, to study other materials as photocatalysts. These can often exhibit greater photocatalytic activity in contrast to TiO_2, for example zinc oxide (ZnO) and bismuth vanadate ($BiVO_4$).[4]

Overall, the photodegradation of plastics is of great interest due to decent efficiencies achieved at ambient temperature and pressure. In addition, it also decreases the time span necessary for following biodegradation, by micro- or living organisms, if desired, and assists full degradation of the synthetic polymers.[34] Though it seems promising, there are aspects which need to be considered for future industrial application. Especially the emission and release of the by-product CO_2, a greenhouse emission gas, and numerous intermediates, can have a negative impact on the environment. The full ramifications are yet to be established. Therefore, the attention has shifted to the rather elegant approach of photocatalytically converting synthetic carbohydrate waste into high-value chemicals and materials, and H_2. This is illustrated in the following chapters.[4]

1.4.2 Simultaneous upcycling and solar fuel production - Photoreforming

In the early 1980s, photoreforming was first reported by *Kawai and Sakata.*[39,40] Inspired by nature's photosynthesis, their first work focused on the conversion of biomass, such as cellulose, into H_2. This was achieved with the assistance of RuO_2/TiO_2/Pt as photocatalyst and the addition of water or a 6M NaOH solution. Upon irradiation with a Xe lamp of 500W, they reported the successful evolution of H_2. In their works to follow, they expanded their investigation from biomass to other organic substrates, such as alcohols, carbohydrates and halogen- and nitrogen-

containing substances. In less than a decade after *Fujisihima and Honda* described their accomplishment in water splitting with a TiO_2 and a Pt electrode[23], *Kawai and Sakata* employed the same semiconductor and noble metal, as co-catalyst, for the conversion of PVC into H_2.[40,41] In principle, photoreforming constitutes of H_2 evolution under anaerobic conditions, by reduction of water molecules, and the simultaneous oxidation of organic substances. Both reactions take place on the surface of a photocatalyst. As depicted in ***Figure 3b***, absorption of sunlight consequently excites an e^- from the VB to the CB, thus reducing water molecules to H_2. The h^+, which remains in the VB, oxidizes organic compounds, i.e. structures containing C, H and O atoms, to CO_2, water and, ideally, high value chemicals. This oxidation step either occurs through a direct or a remote pathway. The latter describes the subsequent formation of •OH from interaction of the h^+ with present water molecules. The ***equations (12)*** – ***(15)*** demonstrate these described mechanistic steps, whereas the ***equations (12)*** and ***(13)*** are identical to the first two steps of photodegradation.[4,39]

$$semiconductor + hv \rightarrow h^+_{VB} + e^-_{CB} \qquad \textbf{(12)}$$

$$h^+_{VB} + H_2O \rightarrow \cdot OH + H^+ \qquad \textbf{(13)}$$

$$2\, e^-_{CB} + 2\, H^+ \rightarrow H_2 \qquad \textbf{(14)}$$

$$h^+_{VB}\ or\ \cdot OH + Plastics \rightarrow Organic\ products + CO_2 \qquad \textbf{(15)}$$

The main difference to conventional photocatalysis for H_2 production, as aforementioned, is organic substrates acting as sacrificial electron donors, also known as hole scavengers. Consequently, the addition of costly compounds such as methanol or EDTA as scavengers is not necessary anymore to enable H_2 production; waste substances, e.g. organic contaminants or microplastics, can be used instead in order to facilitate an effective hole utilisation.[4,21,39]

As mentioned above, photocatalytic water splitting exhibits the drawback of kinetic limitations in respect to the oxidation of water itself. In contrast, photoreforming does not involve this issue. Here, the reforming of the substrate takes place at around equal potential as the H_2 evolution, thus involving a kinetically more facile oxidation. This is yet another great advantage.[4,42]

Moreover, in theory, during a photoreforming process the present organic compound would completely oxidate to CO_2. In reality though, the majority of carbon atoms from the substrate, reside in the produced smaller organic compounds. This is due to incompletion of the reaction sequences. Further, in alkaline media, the CO_2 can be trapped in its mineralised form: carbonate (CO_3^{2-}). This, in consequence, reduces the emission of the greenhouse gas.[42]

This research area has especially gained more attention from around 2017, with a lot of insights from *Erwin Reisner* and his group. In the work from *Wakerly et al.*, CdS quantum dots coated with CdO_x (CdS/CdO_x QDs) were investigated for the photocatalytic valorisation of the natural macromolecules cellulose, hemicellulose and lignin. Herein, the interest was set on a visible light

active semiconductor, ambient conditions and H_2 generation. They were able to generate high rates of the green fuel, as compared to the model photocatalyst TiO_2, without the necessity of a co-catalyst and under strong alkaline conditions.[43] A year later, *Uekert et al.* investigated the same photocatalyst system, but with the focus shifted to the degradation of synthetic organic compounds: PLA, PET and polyurethane (PUR). Additionally it is amongst the first papers establishing a pre-treatment method, which involves hydrolysing the respective substrate in an alkaline solution, like NaOH, for 24 hours and by applying minimal external heating to 40°C. After filtration, the supernatant is then used as substrate for the subsequent photoreforming reaction. This is said to considerably boost the activity of the process as the substrate has already been broken into smaller fragments.[44]

Many works have followed since, investigating different photocatalyst systems and various plastics. A common denominator: the employment of a pre-treatment in alkaline solution.

At the end of 2022, *Du et al*. reported a Janus particle as photocatalyst, comprised of a CdS nanorod tipped with MoS_2. The nanorod aimed the oxidation of the organic substates PET and PLA, as it functioned as the light absorber and hole acceptor. The tip encouraged the collection of e^- and thus the HER. Interestingly, this paper also successfully upcycled the polyolefin LDPE as a substrate, which appeared novel.[45] Several other papers were unsuccessful in doing so or could only achieve minimal oxidation, hence often focusing on PET or PLA.[46,47]

From present literature it can be concluded, that the majority of publications of this field are strongly focused on the employment of visible light active photocatalysts. This involves the semiconductors mentioned above, but also the application of various co-catalysts. Although Pt appears to be the most popular[30,40,41,47], further co-catalysts include Co[43], NiP[48] and Ni_2P[46]. As a consequence, the presented studies rely on solar simulated irradiation, rather than UV light sources.[43,45–47,49]

Many publications discuss similar methodologies for the photoreforming process itself, but with the focal point on the characterisation of the presented photocatalyst. In general, the most common reaction medium is an alkaline solution of various concentrations (0,5M - 10M), either NaOH or KOH. However, H_2O has also been investigated thus far.[40,41,43,47,50] As aforementioned, the alkaline media is believed to promote hydrolysis of the substrate and thus expedite the photoreforming process. Regarding temperature, a majority of literature focuses on room temperature valorisation, which would be the most attractive for an industrial application, as it would be more cost-efficient.[48,50,51] On the other hand, temperatures of 40°C - 70°C were rarely studied, if the focus was shifted to the impact of exalted temperatures.[30,47,52] Concerning scale or duration of the experiments the selected parameters are diverse. Whilst some studies investigate very small volumes, of 7 mL for example, other works conduct their experiments with larger setups of up to 280 mL.[40,41,48,52] Also regarding irradiation periods no clear standard can be concluded, as they vary from 2 - 120 hours, if long-term experiments are carried out. Over the years, a number

of gas- and liquid-phase products have been reported, depending on the substrate under investigation. Whilst cellulose forms smaller saccharides[43], PUR is known to produce lactate, formate and acetate[44] and the upscaling of PLA results in carbonate[46], for example. When the gaseous products are investigated, the focus is predominantly set on H_2 [47–49,51], which presents a viable alternative to fossil fuels. Further products which have been reported include CO and CO_2[30,47,48,53], but also small amounts of ethanol and methanol[40] and propane and ethane[45].

Another potential product from photoreforming of plastics, such as PE, is methane (CH_4).[45] This compound is often negatively discussed, as it is a greenhouse gas contributing to global warming. A majority of CH_4 emissions are anthropogenic, produced through agriculture, cattle farms and fossil fuels.[54] Although the negative impact on the environment is well-known, omitting CH_4 completely would not be feasible, as it is substantial for the production of many different crucial chemicals. A prime example would be steam reforming CH_4 with water, producing H_2 and carbon monoxide (CO). This gaseous mixture is also known as “syngas”, which is of utmost importance as feedstock for fuels and numerous high-value compounds.[55]

Overall, the concept of photodegradation presents a viable alternative and sustainable opportunity for the disposal of plastic waste. However, it requires the utilisation of organic solvents and the full impact of the intermediates and products on the environment are yet to be investigated. In contrast, the approach of photoreforming is showing promising results and entails the upcycling of plastic waste, whilst simultaneously generating green H_2. Both aspects are imperative for a more environmentally friendly approach in energy and waste management. This in consequence would beneficially contribute to the issue of global warming and support the phasing out of fossil fuels.

2. Motivation and Aims

As elucidated in the previous chapters, many efforts have been made in the past decades, investigating the principles and possible applications of photocatalysis, predominantly water splitting, to obtain green H_2. The scientific community regard it as an auspicious opportunity for a zero-emission alternative to fossil fuels, which are a limited resource and detrimental to the environment. Since the field of photocatalysis has grown, many other possible applications have been discussed Recently, a great interest has arisen towards photoreforming, which targets simultaneous generation of solar fuels with the upcycling of organic macromolecules, such as microplastics. If successful, this could not only produce fuels in a sustainable manner, but also be a desirable solution for the recycling and discarding issue of everyday plastics, like PET bottles or PE bags.

The main focus of this work was the study of impact of selected *(1) photocatalyst*, *(2) atmosphere*, *(3) temperature* and *(4) substrates* on the photoreforming process.

(1) Herein both neat P25-TiO_2 and with Pt as co-catalyst, were employed in the conducted experiments for the purpose to establish the setup and evaluation methods, as it is a very well-studied photocatalytic system, especially in the terms of water splitting. It was also the first photocatalyst implemented in the simultaneous oxidation of various carbon species, as was reported by *Kawai and Sakata* in 1981.[41]

(2) Regarding atmosphere as a parameter under investigation, experiments were conducted with the addition of air (CA), to further encourage oxidation and subsequent formation of liquid compounds, i.e. *photodegradation*, or under inert conditions with He, to study the generation of gaseous products, i.e. *photoreforming*.

(3) Concerning temperature, the respective samples were either irradiated at room temperature (RT) or heated to 70°C. In previous work, conducted by *Nagakawa and Nagata*, it was described that under sunlight the reaction solution was heated to 70°C, without external assistance. The increase in temperature consequently promoted both the generation of H_2 and the hydrolysis of the investigated substrates.[47]

(4) As it was of interest to consider diverse chemical structures, PET, PP and LDPE were selected. It has been reported that PET, a polyester, has shown promising degradation results in a number of works so far.[30,42,44–46,50] However for the polyolefins, PP and LDPE, success is yet to be achieved.[44,46]

A number of papers have reported the beneficial impact of pre-treatment to the photoreforming process, as has been elaborated above.[30,42,44–46] To include this pre-treatment to a certain degree, 1M NaOH was chosen as reaction medium. It is believed that irradiation under the alkaline condition supports the hydrolysis and subsequent photoreforming of the investigated compounds.[44,46]

With future possible technological application in mind, it was also of interest to investigate the quantity of solar fuels and upcycling products obtained due to irradiation with a solar simulator. This idea was inspired due to one of the main goals of photocatalysis being the utilisation of sunlight, a rich and inexpensive energy source.[56] In addition, a minor upscaling of the established setup was executed, to further evaluate feasibility in an industrial scale.

3. Materials and Methods

3.1 Applied chemicals

During the course of this project the following chemicals, shown in ***Table 1***, were implemented in this work. These include the photocatalyst components, substrates used for the oxidation reaction, the reaction medium itself and standard solutions for subsequent characterisation. All compounds were commercially obtained and no additional purification steps were carried out before use.

***Table 1**: Summary of applied compounds.*

Chemical formula	Name	CAS number	Purity	Supplier	Purpose
TiO_2	Titanium(IV)oxide, P25	13463-67-7	-	Acros Organics	Photocatalyst (support)
H_2PtCl_6	Hydrogen hexachloroplatinate (IV)	16941-12-1	-	Fluka (Sigma – Aldrich)	Pt precursor
CH_3OH	Methanol	67-56-1	Absolute (≥99,9%)	VWR	Photodeposition of Pt
NaOH	Sodium hydroxide	1310-73-2	≥ 99,0%	Carl Roth	Reaction medium
$(C_{10}H_8O_4)_n$	Polyethylene Terephthalate	26038-69-9	99,0%	Nanochemazone	Substrate
$(C_2H_4)_n$	Low Density Polyethylene	9002-88-4	99,0%	Nanochemazone	Substrate
$(C_{10}H_8O_4)_n$	Polyethylene Terephthalate	26038-69-9	-	Provided by CHASE center	Substrate
$(C_3H_6)_n$	Polypropylene	9003-07-0	-	Provided by CHASE center	Substrate
$C_2H_6O_2$	Ethylene glycol	107-21-1	99,5%	Acros Organics	Standard solution for HPLC
$C_2H_2O_4 * 2H_2O$	Oxalic acid dihydrate	6153-56-6	99,0%	Sigma-Aldrich	Standard solution for HPLC
CH_3COOH	Acetic acid	7732-18-5	98-100%	Fisher Scientific	Standard solution for HPLC
CH_2O_2	Formic acid	64-18-6	85,0%	Riedel-de Haën	Standard solution for HPLC
H_3PO_4	Ortho-phosphoric acid	7664-38-2	85,0%	PanReac AppliChem - ITW reagents	Neutralization of samples

3.2 Conducted characterisation methods

As aforementioned, the investigation of both the gaseous and the liquid products were the aim of this work.

Gas chromatography (GC) is a popular analytical method for the investigation of sample composition and quality, but also implemented as a purifying technique when required. Herein, the mobile phase is a carrier gas in which the sample gets injected. In the case of a liquid sample, vaporisation takes place in a heated injector. The gaseous mixture then flows through a very long and slim capillary, which possesses an internal coating as stationary phase. As the sample vapours distribute between the two phases, whilst passing through the column, the eluted products are then collected by a detector. As a result, the information of interest can be concluded from a gas chromatogram, which entails peaks of characteristic retention time for each specific product.[57] In the course of this project a GC, of the model Shimadzu Nexis GC-2030 BID, was employed to analyse gaseous products from the samples. Hereby, the equipment was calibrated to detect H_2 and CH_4, but also CO_2 and CO. For each measurement 200 µL of sample was obtained from the headspace of the vial, injecting it immediately after extraction. The ppm values were then calculated to µmol or µmol/h by applying ***equation 16*** converted to ***equation 17***.

$$p * V = n * R * T \rightarrow n = \frac{p*V}{R*T} \qquad \textbf{(16)}$$

$$\mu mol = \frac{concentration\ [ppm] * headspace\ [mL] * 10^{-6} * p\ [Pa]}{R\left[\frac{m^3 * Pa}{mol * K}\right] * T\ [K]} \qquad \textbf{(17)}$$

p ... $101325\ Pa$

R ... $8{,}314\ m^3 * Pa / mol * K$

T ... $298\ K = 25\ °C;\ 343\ K = 70°C$

High pressure liquid chromatography (HPLC) is a widespread separation method, which is utilized to determine liquid chemical compounds and can analyse samples comprised of both high and low molecular weight components. Herein a liquid mobile phase, the sample and an appropriate solvent, passes through a column of a solid stationary phase. The components, of the sample under investigation, are then separated due to different factors, such as chemical structure and nature, but also their molecular weight. As there is a wide range of different HPLC techniques available, both quantitative as well as qualitative information can be attained from complex mixtures.[58] In this work, the data was acquired with a setup from Shimadzu and a refractive index detector (RID-20A) of the company, in collaboration with CEST. In order to gain

insight on the oxidation products, standard solutions of expected compounds and of the concentrations 10 mg/mL,1 mg/mL and 0,1 mg/mL were first prepared. These included formic acid (FA), acetic acid (AA), ethylene glycol (EG) and oxalic acid (OA). Each standard solution was prepared by dilution or dissolving of the respective compound in deionised water. For the measurement of the samples, 2 mL of the respective solution was transferred to a new vial and the pH was then altered from strongly alkaline (pH 12) to neutral or acidic conditions (pH 7 - 2). This step was carried out with H_3PO_4, as this acid would then be employed as eluent for the subsequent analysis. To avoid any particles present in the sample, each solution was additionally filtered with a syringe filter. Each standard solution was analysed three times, to then conclude the calibration curve of the methodology and every sample was measured twice. The injection volume for each measurement was 10 µL.

4. Experimental part

4.1 Photodeposition of the co-catalyst

To implement 1 wt.% of Pt as co-catalyst on TiO_2, 1g of P25 was dissolved in 100 mL MeOH and 100 mL of deionised H_2O, in a 500 mL round bottom flask. Then 12,5 mL of the precursor (H_2PtCl_6) was added to the solution. The photodeposition took place with two deep UV light sources (Lumatec lamp and LED lamp), with a wavelength between 190-400 nm and for around 2 hours, whilst stirring the solution with a magnetic stirrer. Afterwards the solvent was removed with a rotary evaporator and the remaining solid was dried in the vacuum oven overnight at 60°C. The resulting product is referred to as P25-Pt.

4.2 General procedure of the experiments

The objective of this work, as aforementioned, was the comparison of photocatalytic activity of neat P25 in contrast to P25-Pt, and the effect of temperature and atmosphere on the photoreforming process. Herein, the reactions were carried out either under ambient conditions at room temperature (RT), i.e. around 25°C, or at 70°C. In regards to the reaction atmosphere, He was of interest for inert conditions and the investigation of solar fuel generation in the gas phase. In contrast, compressed air (CA) was employed to support the microplastic oxidation and for the subsequent study of photoreforming products in the solution.

To begin with, a preliminary set of experiments was conducted with various combinations of the parameters mentioned above. This also included some blank experiments and repetition of selected samples. The latter was carried out to estimate the error of the methodology, regarding sample preparation, timing of each step, position of the reactor, weighing of the constituents, insufficient purging of the solution and loss of liquid and photocatalyst during transfer from one vial to another, for example. The calculated standard deviations (SD) are also applied to subsequent samples, as can be observed from the figures in the next chapters. Moreover, different types of microplastics (PET, LDPE, PP) and sources were compared. Afterwards, other setups were investigated, such as upscaling of the experiment, prolonged irradiation or a different light source.

4.2.1 Main and blank experiments

For each experiment, 18 mg of microplastic (1 mg/mL) and 9 mg of the respective photocatalyst (0,5 mg/mL) were each suspended in 9 mL of 1M NaOH. The sample vial, a 20 mL glass vial with a septum, containing the microplastic under investigation, was sonicated for 10 minutes. The photocatalyst was sonicated for 1 minute in the case of neat P25 and for 2 minutes when P25-Pt was employed. Once the respective photocatalyst was suspended well, it was transferred to the microplastic solution and the reaction solution was sonicated for another minute.

The reaction solution was then purged for 10 minutes, either with CA, if the liquid products were the main focus (photodegradation), or He, in the case of gaseous solar fuel generation being investigated (photoreforming). For the former, the 5 hour irradiation of the sample took place, whilst still continuing the addition of CA to the reaction solution, to ensure constant concentration of O_2 in the vial. In contrast, for experiments conducted with the latter conditions, the system was closed after the purging period and no additional gas flow took place during irradiation. In order to study the gaseous products of the photocatalytic reaction, a GC sample was taken before and right after irradiation of the respective sample. GC sampling was only conducted for He-based samples. After 5 hours of illumination, every sample was filtered. The solid product was washed with deionised water and then dried in a drying oven overnight at around 60°C. To monitor the extent of degradation of the respective microplastic, the weight of the solid product was documented after drying. Both the solution and the dried filter cake were kept for future characterisation. This filtration step is displayed in ***Figure 4-6***.

This procedure was carried out for all main and blank experiments, but also whilst investigating other microplastic species.

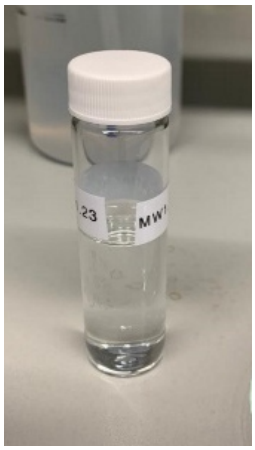

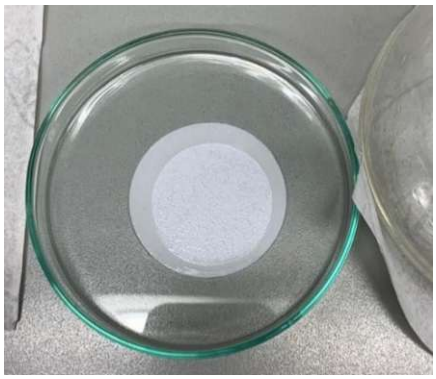

Figure 4 *(left)**:** Used filtration setup;* ***Figure 5*** *(middle)**:** filtered product solution in the vial;* ***Figure 6*** *(right) solid product on the filter paper before drying, from a sample comprised of neat P25 and PET.*

In general, the setup was comprised of a UV-light source, an LED lamp centred at 365 nm in wavelength and 0,219 W in power (measured at a distance of 15 cm), a heating plate with an integrated magnetic stirrer and two gas lines, one for CA and the other for He. No cooling system was introduced to the setup. The images below, ***Figure 7***, ***8*** and ***9***, show the established experimental setup used for all experiments, with the exception of samples irradiated with the Xe lamp.



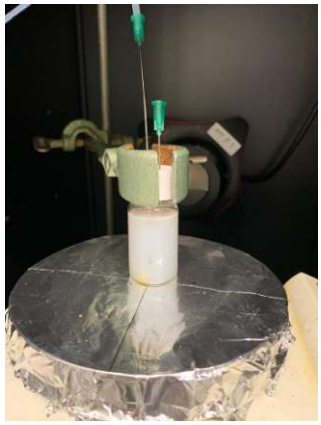

Figure 7 *(left)**:** workplace used for all experiments with a UV lamp – lovingly named Betsy;* ***Figure 8*** *(middle)**:** established setup, with markings for replicable results;* ***Figure 9*** *(right)**:** 20 mL glass vial containing sample and purging with He, distance between sample and lamp is 15 cm.*

4.2.2 Additional experiments

For the experiments conducted with a solar simulator (Xe lamp with an IR-filter, 0,067 W in power) or in an upscaled manner, the general procedure remained indifferent to the description above. In the case of the former, the same vial was used, but a sample volume of 16 mL rather than 18 mL was prepared, with the same concentration of the substrate PET (1 mg/mL) and of the photocatalyst (0,5 mg/mL). The purging of the solution took place in the same workplace, as was used for irradiation with a UV lamp, before transferring it to the other setup. In addition, the irradiation period of 5 hours was increased to 24 hours, as it was expected that the photocatalytic activity of P25 would not be as high as for UV illumination. For the latter, upscaling of the setup, a 100 mL round bottom flask was utilised. Again, the general procedure, with a UV lamp, was equivalent to the aforementioned method, but the reaction volume was increased to 100 mL, sonication time of the components was increased when necessary and the solution was purged with He for 30 minutes. Additionally, the irradiation of the reaction solution took place for 32 hours and samples were taken every hour in the first 5 hours and every 2 hours between hour 24 and 32. For these two sets of experiments, it was of interest to compare the influence of neat P25 with external heating (at 70°C) to P25-Pt at RT. It is to be noted, that no external cooling was applied and for the upscaled experiment no oil bath was used, as this might have blocked or limited the

exposure to the light source. Therefore, there might have been a temperature gradient within the solution.

The experimental arrangements for the two experiments with a Xe lamp are demonstrated in ***Figure 10*** and ***11***.

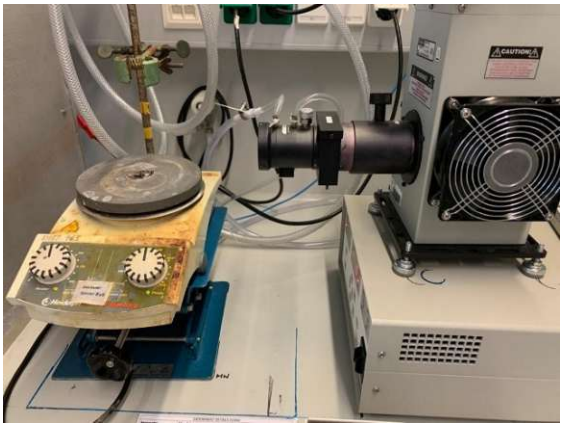

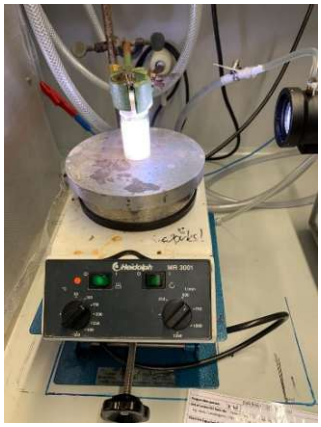

Figure 10 *(left):experimental setup for the solar simulated irradiation with a Xe lamp (including an IR-filter), with a distance between sample and lamp of 15 cm;* ***Figure 11*** *(right): Illumination of the sample.*

In the following images, ***Figure 12*** and ***13*** the round bottom flask of the upscaled experiments is illustrated.

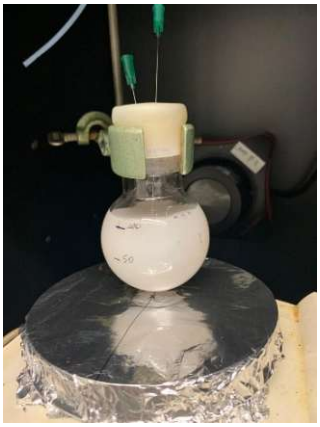

Figure 12 *(left):purging of the solution, distance of sample to the lamp is 15 cm;* ***Figure 13*** *(right): distribution of UV light beam on the enlarged volume.*

4.3. Prepared samples

The following table (***Table 2***) displays an overview of the scheme followed for the samples prepared in the course of this work. The sample name is comprised of "x", which describes the microplastic under investigation, as can be concluded from ***Table 3***, the photocatalyst, either neat P25 or with Pt as co-catalyst (P25-Pt), the atmosphere and temperature of the reaction. In the case of experiments taking place in an upscaled manner, with a light source other than a UV lamp or an extended irradiation period, the sample name contains the suffix "UP" (upscaled), "SS" (solar simulator) or "24h". Additionally to this, some blank experiments were also executed. These samples include "D" for "dark", i.e. no irradiation, "NM" for "no microplastic" or "NC" for "no catalyst", at the end of the sample name.

Table 2: *Chosen parameters for each sample.*

Experiment number	Sample name	Photocatalyst	Atmosphere	Temperature [°C]
A	x/P25-Pt/CA/RT	P25-Pt	CA	RT
B	x/P25/CA/RT	P25	CA	RT
C	x/P25-Pt/He/RT	P25-Pt	He	RT
D	x/P25/He/RT	P25	He	RT
E	x/P25-Pt/CA/70°C	P25-Pt	CA	70°C
F	x/P25/CA/70°C	P25	CA	70°C
G	x/P25-Pt/He/70°C	P25-Pt	He	70°C
H	x/P25/He/70°C	P25	He	70°C

Table 3: *Description of x and the corresponding substrate.*

x	Microplastic
1	PET (source 1)
2	PET (source 2)
3	LDPE
4	PP

A summary of all samples, discussed in the following sections, is demonstrated in ***Table 4***, describing sample name, substrate under investigation, applied light source and characterisation method operated for analysis of the liquid or/ and gaseous products.

Table 4: *Outline of all produced samples.*

Experiment number	Sample name	Substrate	Light source	Characterisation method
Main experimental series for substrate 1				
A	1/P25-Pt/CA/RT	PET (source 1)	UV lamp	HPLC
B	1/P25/CA/RT	PET (source 1)	UV lamp	HPLC
C	1/P25-Pt/He/RT	PET (source 1)	UV lamp	GC
D	1/P25/He/RT	PET (source 1)	UV lamp	GC
E	1/P25-Pt/CA/70°C	PET (source 1)	UV lamp	HPLC
F	1/P25/CA/70°C	PET (source 1)	UV lamp	HPLC
G	1/P25-Pt/He/70°C	PET (source 1)	UV lamp	GC, HPLC
H	1/P25/He/70°C	PET (source 1)	UV lamp	GC
Blank experiments				
C	1/P25-Pt/He/RT/D	PET (source 1)	-	GC
C	1/P25-Pt/He/RT/NC	PET (source 1)	UV lamp	GC
C	P25-Pt/He/RT/NM	-	UV lamp	GC
Additional experiments				
C	1/P25-Pt/He/RT/UP	PET (source 1)	UV lamp	GC, HPLC
C	1/P25-Pt/He/RT/SS	PET (source 1)	Xe lamp	GC, HPLC
H	1/P25/He/70°C/UP	PET (source 1)	UV lamp	GC, HPLC
H	1/P25/He/70°C/SS	PET (source 1)	Xe lamp	GC, HPLC
H	1/P25/He/70°C/24h	PET (source 1)	UV lamp	GC,HPLC
Alternative microplastic sources				
C	2/P25-Pt/He/RT	PET (source 2)	UV lamp	GC
C	3/P25-Pt/He/RT	LDPE	UV lamp	GC
C	4/P25-Pt/He/RT	PP	UV lamp	GC

5. Results and discussion

5.1 Proof of concept and blank experiments

To begin with, a set of blank experiments were performed, to prove the concepts of photoreforming and to verify that the desired reduction reaction – hydrogen evolution – can be accomplished. Herein, the experiments were carried out under ambient conditions at RT, with P25-Pt as photocatalyst and PET as substrate. The first sample contained both PET and P25-Pt (experiment C from the main series in ***Table 4***). For comparison, the blank experiments only contained either the microplastic or the photocatalyst or both but did not entail illumination (blank experiment series in ***Table 4***). The results for the amounts of generated H_2 is depicted in ***Figure 14a***.

The presented data obtained for *1/P25-Pt/He/RT* (experiment C) demonstrates successful photoreforming, as indeed H_2 was generated (around 1,15 µmol/h). When comparing the results attained for the sample to the three blanks, it can be concluded that the presence of both the photocatalyst and the light, are vital for a successful photoreforming process.

As previously mentioned, literature hitherto has merely focused on the generation of H_2 and has thus not reported CH_4 production. However, a significant quantity was detected by the GC throughout this project. Therefore this compound is being discussed as well.

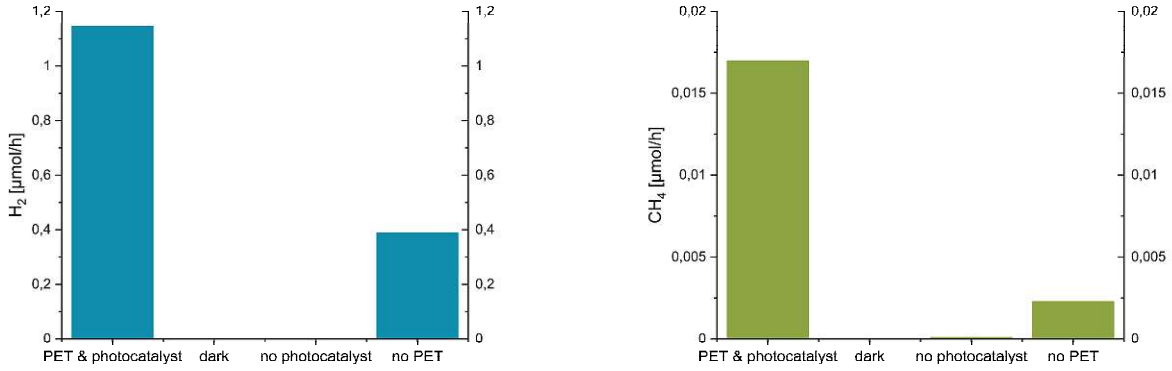

Figure 14a *(left): H_2 generation of different blank experiments;* ***Figure 14b*** *(right): CH_4 generation of different blank experiments; "PET & photocatalyst" describes 1/P25-Pt/He/RT, "dark" (1/P25-Pt/He/RT/D) is the same but without irradiation, "no photocatalyst" (1/P25-Pt/He/RT/NC) shows the sample solely comprised of PET and "no PET" (P25-Pt/He/RT/NM) depicts the experiment without microplastic.*

Regarding CH_4 (***Figure 14b***), 0,017 µmol/h were obtained for *1/P25-Pt/He/RT*. In contrast, the samples which were not irradiated or did not contain any photocatalyst, did not result in the production of neither H_2 nor CH_4. Although ***Figure 14b*** shows a very small bar for *1/P25-Pt/He/RT/NC*, the value is ascertained as zero, as the measured 6 ppm are minor and outside of the calibration range of the GC.

In terms of photocatalysis, both figures demonstrate the requirement of light irradiation, as photons are essential for the exciton generation, and the presence of a photocatalyst, to successfully achieve the photocatalytic reduction from water to H_2 and of the substrate to CH_4.
In the experiment comprised solely of 1M NaOH and P25-Pt (*P25-Pt/He/RT/NM*), a mere quantity of 0,002 µmol/h of CH_4 was generated, equating to around 6 times less than in the case of the sample containing PET. In a study from 2018, by *Royer et al*., the impact of light irradiation on diverse types of plastic and the subsequent generation of CH_4 and other gaseous hydrocarbons was studied. They showed that ambient solar radiation is sufficient to produce a measurable quantity of CH_4 from numerous substrates, including PP, but also PET and polycarbonate (PC). A more extensive study was made with LDPE, investigating the impact of different spectral ranges, including the entire solar spectrum of 280-700 nm and UV-B irradiation of 320-700 nm.[59] Therefore it is believed to be a possibility that some CH_4 may have been produced from the PP cap of the employed glass vial, as no other reactive organic substrate was present during this experiment. However, contamination of the commercially obtained P25 cannot be entirely excluded and thus could have acted as a carbon source. Nonetheless, the exact origin of this gaseous product is uncertain and further investigation is required.
Concerning H_2, 0,389 µmol/h was produced, which is equivalent to approximately 33% of H_2 formed in the case of *1/P25-Pt/He/RT*. It is feasible that this H_2 may originate from direct water splitting, triggered by P25-Pt, as no microplastic or other H^+ - source was present in the reaction solution. On the other hand, it is not impossible for PP, from the vial's cap, to act as a H^+ donor, which could thus in addition aid H_2 generation.
Moreover, both ***Figure 14a*** and ***14b***, demonstrate a direct correlation between the production of both H_2 and CH_4. The more H_2 is formed, the less CH_4 can be detected at the end of the experiment. This suggests that CH_4 may be an intermediate of the former.

5.2 Experimental series with PET

After establishing the methodology, experiments were carried out with the focus set on PET as a substrate and the investigation of influence of temperature and photocatalyst on the generation of the respective solar fuel. Within this section, the analysis of the gaseous phase and the performed gravimetry are evaluated. The results from the microplastic oxidation will be included in a later chapter.

5.2.1 Effect of co-catalyst and reaction temperature

The results discussed in this chapter involve experiments carried out after purging with He and with UV irradiation (experiments C, D, G and H from main series, ***Table 4***). The ***Figures 15*** and ***16*** demonstrate the generation of H_2 and CH_4, either with or without the presence of Pt as co-catalyst. In addition, the effect of elevated temperature is studied as well.

As can be seen in ***Figure 15***, both elevated temperature and the presence of co-catalyst appear highly beneficial in the H_2 evolution. The highest quantity of H_2 within this experimental series is achieved for both the RT and 70°C sample containing the co-catalyst under investigation. The exact value for the former is 1,15 µmol/h, as was stated above. In the case of the 70°C sample, the measured value was estimated at 100 000 ppm (10% of the head volume), as the actual detected amount was not within the calibration range of the GC, but rather greater. This approximated quantity corresponds to at least 1,42 µmol/h and is equivalent to at least around 23,5% increase solely due to a raise in temperature. Conversely, the absence of Pt results in a H_2 value close to zero at RT and a very poor increase in H_2 production to 0,036 µmol/h (drop of 39 times compared to P25-Pt), when the solution is heated to 70°C. In regards to H_2 evolution, this is not very surprising, as aforementioned TiO_2 with Pt is a very well-studied photocatalytic system and has concluded promising results for decades. In previous work by *Nagakawa and Nagata*, the beneficial impact of exalted temperature was reported, however not to such extent.[47]

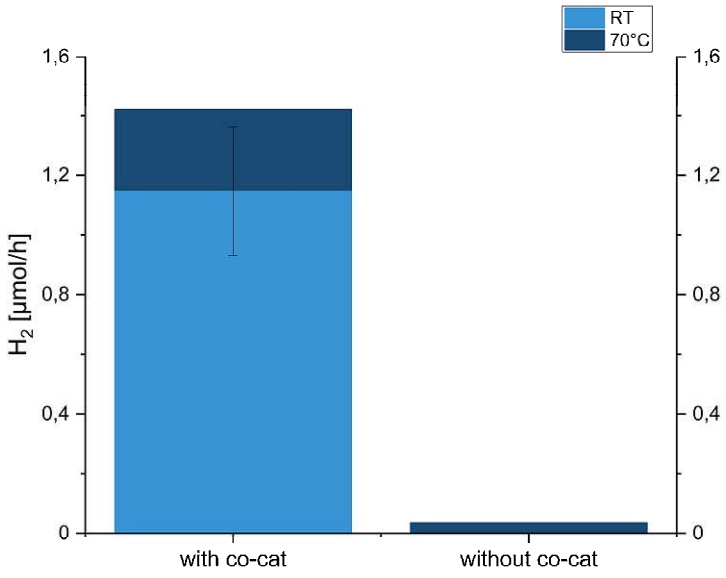

Figure 15: *H_2 generation influenced by temperature and presence of co-catalyst; 1/P25-Pt/He/RT – with co-catalyst and at RT, 1/P25-Pt/He/70°C – with co-catalyst at 70°C; 1/P25/He/RT – neat P25 and RT; 1/P25/He/70°C – neat P25 and 70°C; SD ± 18,8% with co-catalyst; SD ± 19,3% without co-catalyst.*

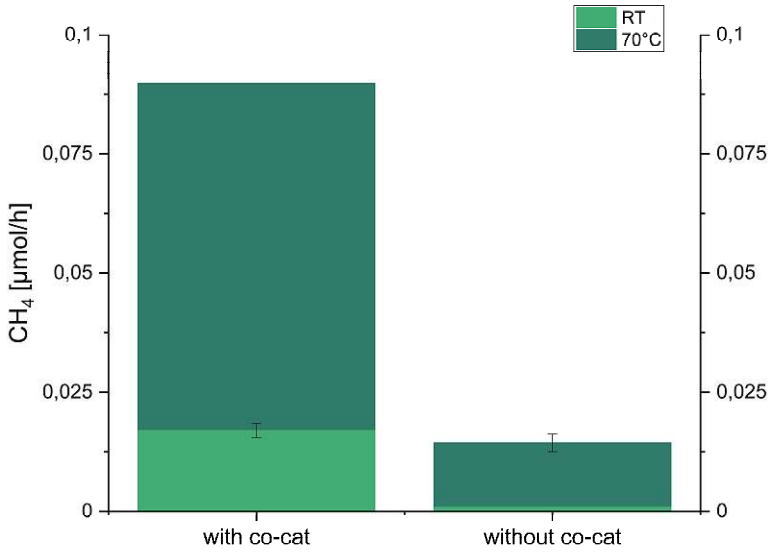

Figure 16: *CH_4 generation influenced by temperature and presence of co-catalyst; 1/P25-Pt/He/RT – with co-catalyst and at RT, 1/P25-Pt/He/70°C – with co-catalyst at 70°C; 1/P25/He/RT – neat P25 and RT; 1/P25/He/70°C – neat P25 and 70°C; SD ± 8,7% with co-catalyst; SD ± 12,7% without co-catalyst.*

The results for the CH_4 production demonstrate a trend similarly to H_2, as is depicted in ***Figure 16***. Overall, a substantial elevation in CH_4 formation is shown in the case of P25-Pt, in contrast to neat P25. Interestingly, a much greater increase, as consequence of enhanced temperature to 70°C, can be obtained from the present results, when comparing to H_2. Moreover, this is equivalent to 3 times more CH_4 than what was found at RT. For the samples comprised of neat P25, the application of 70°C leads to a 16 times greater production in the greenhouse gas, with a surge from 0,0009 µmol/h to 0,014 µmol/h.

Taking the feasibility in future industrial technology into consideration, the results underline strong benefit of both elevated temperature and the employment of a co-catalyst, to obtain the best photoreforming results. This is especially the case if H_2 generation is targeted. However, although much lower values are achieved with neat P25, it could yet be of interest for the synthesis of CH_4, as notable quantities have been detected. Both photosystems seem to have promise and their industrial application would depend strongly on the cost-productivity trade-off relevant to the specific use scenario.

5.2.2 Gravimetric study

As described in *4.2.1 Main and blank experiments*, subsequent to each photocatalytic experiment, the reaction solution was separated from the solid remains, of the substrate and the photocatalyst, through filtration. After drying the solids, the weight was documented, to assess the degree of substrate degredation to CO_2, liquid- or gas-phase products. The following images, ***Figure 17***

and ***18***, summarize the results for the preliminary samples comprised of PET (source 1) and purged with CA as well as He, with the exception of *1/P25-Pt/He/RT*. The values shown, refer merely to the remaining mass of the substrate, as the photocatalyst is not consumed during the photoreforming process.

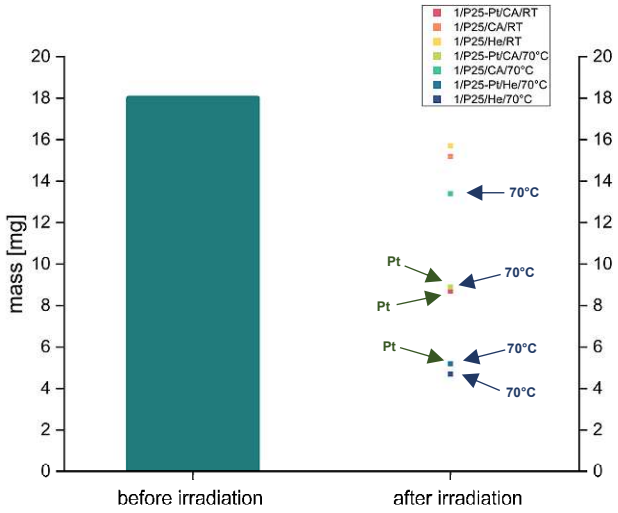

Figure 17: *Mass of PET before and after irradiation (in mg); each sample was comprised of 18 mg of microplastic before illumination with a UV lamp; investigated samples and respective conditions illustrated in the legend.*

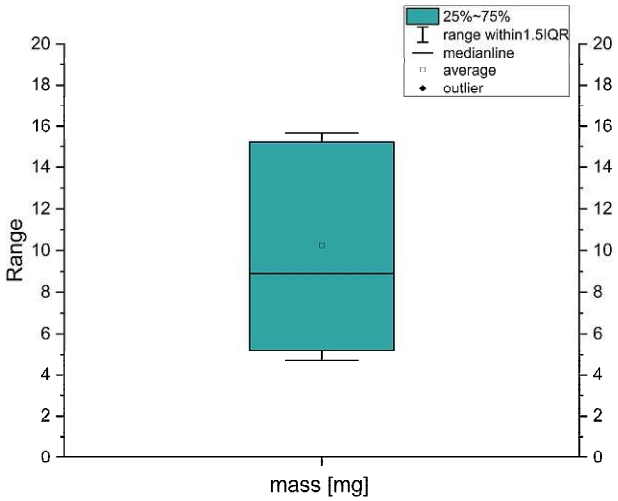

Figure 18: *Box plot diagram of the displayed values in* ***Figure 17****; the depicted data set ranges from 4,7 mg to 15,7 mg and the calculated average is 10,3 mg;. no outliers are present.*

The highest degree of microplastic degredation is exhibited by both of the samples, which were purged with He and illuminated at exalted temperature (*1/P25-Pt/He/70°C* and *1/P25/He/70°C*). Moreover, the sample containing neat P25 displays the lowest remaining mass of 4,7 mg, which is equivalent to 74% mass depletion. Conversely, both CA samples, which contain the co-catalyst (*1/P25-Pt/CA/RT* and *1/P25-Pt/CA/70°C*), display a remaining mass of 8,7 mg at RT and 8,9 mg

at 70°C. From this, it can be concluded that again, an increase in temperature aids the photoreforming process. Furthermore, the two samples irradiated at RT and without Pt (*1/P25/CA/RT* and *1/P25/He/RT*), display approximately identical values under both oxygen-rich and inert conditions. Finally, *1/P25/CA/70°C* remained with a mass of 13,4 mg, thus displaying the third lowest degree of oxidation obtained within this series of experiments.

The presented results appear contradictory to the prediction that the employment of CA would expedite the oxidation process. As the contribution of additional oxygen should generate more ROS than under inert conditions, it was believed that this would subsequently lead to higher rates of substrate oxidation. However, this was not necessarily the case. As aforementioned, both He samples irradiated at 70°C, concluded in the highest degree of degradation.

Moreover, the presence of Pt appears more beneficial in terms of degradation of the microplastic. As aforementioned, co-catalysts are implemented to aid the reduction reaction of the photocatalytic process. Therefore, the system can consume more e^- and this further leads to less recombinations occurring. In consequence, more h^+ are available for the oxidation processes. This emphasizes the favourable outcome achieved with the presence of Pt.

However, it appears that in an inert atmosphere and with an increase in temperature (in contrast to CA and RT), more promising results are accomplished, especially when neat P25 is employed as photocatalyst. Contrary to general expectation that oxiygen radicals are the main species responsible for oxidation during the photoreformin process, *Uekert et al.* were able to conlcude this not being the case. Herein, they investigated the present oxidation mechanism with therephthalic acid as •OH scavenger. The results of this study showed that h^+ transfer between the photocatalyst und investigated substrate is indeed the dominant present pathway.[46]

As described by the kinetic theory, an exalted temperature aids the oxidation of the substrate. By providing the system with additional energy, due to increase in temperature, the molecular species are promoted to overcome the thermodynamic activation barrier. This subsequently expedites the reaction, in this case the oxidation. Furthermore, temperature is also an important parameter in respect to molecular collisions. The number of collisions are further exalted by providing the molecules with more energy.[60]

In general, this outcome accentuates the beneficial influence of an inert atmosphere, as well as an enhancement in temperature, in respect to the oxidation of the substrate. CA requires the presence of Pt for the best results. Nonetheless, these conditions lead to a mere 52% in mass depletion from the initial 18 mg. Overall, the obtained results suggest that the oxidation of the microplastic predominantly takes place via direct h^+ transfer, rather than through the assistance of ROS, as the most promising values were attained with He.

5.2.3 Reproducibility of results

Once all conceivable alterations of the discussed parameters under investigation were conducted (***Table 4***, main series), it was further of interest to study the reproducibility of selected samples, which in turn suggest the reliability of the established setup and evaluation methods.
Herein, *P25-Pt/He/RT/NM* (blank experiment from ***Table 4***) was carried out three times, as is illustrated in ***Figure 19***. Further, *1/P25/He/70°C* (experiment H from main series, ***Table 4***) was also repeated three times. This, on the other hand, is displayed in ***Figure 20***. Both images include the calculated mean averages of the respective samples and the corresponding SD. As aforementioned, the obtained SD were applied to other samples discussed, to assess the error in the established methodology. Some possible error sources may for instance be related to sample preparation, error in volume of the reaction solution drawn by the pipette or injection into the GC.

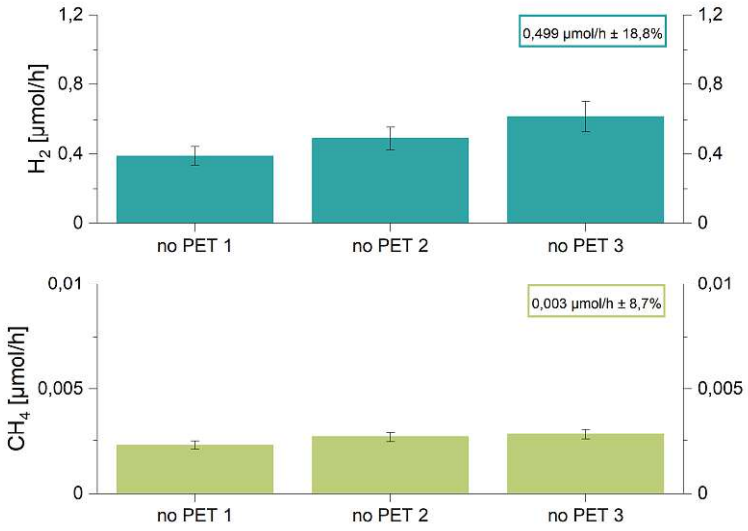

Figure 19: *Measured values of H_2 (top) and CH_4 (bottom) of P25-Pt/He/RT/NM sample 1-3; each compound shows the calculated mean average and respective SD, which is also included in each bar of the diagram.*

From the results of *P25-Pt/He/RT/NM,* in ***Figure 19***, it can be deduced, that the detected quantities are qualitatively comparable throughout all three executed experiments. As is summarized in the image, the measured values of H_2 conclude a mean average of 0,499 µmol/h and a SD of 18,8%. On the contrary, the mean average of CH_4 is 0,003 µmol/h and the SD, showing a decrease of approximately 10%, is a mere 8,7%. In other words, these results suggest, that around 0,5 µmol/h of H_2 might be formed from direct water splitting of P25-Pt and 1M NaOH. In addition, solely 0,003 µmol/h of CH_4 is produced, presumably from the irradiation of the vial's PP cap, as was hypothesized above. Nonetheless, the exact mechanism of both H_2 and CH_4

formation has not been studied and is therefore unclear. Overall these obtained values are indeed reproducible.

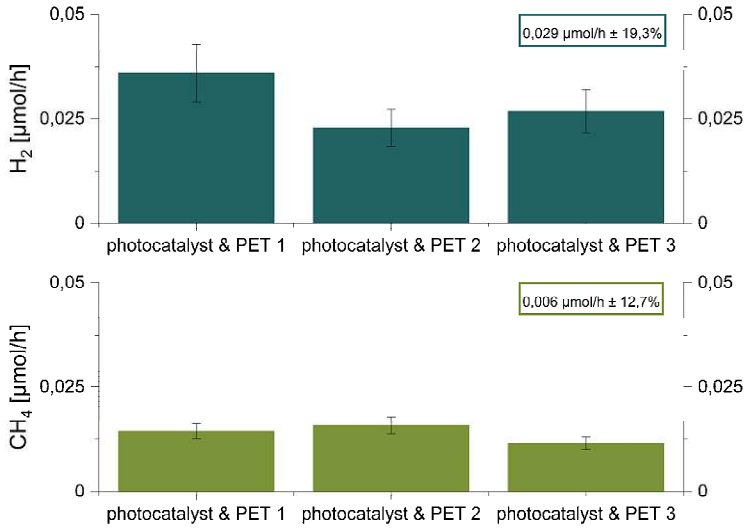

Figure 20: *Measured values of H_2 (top) and CH_4 (bottom) of 1/P25/He/70°C sample 1-3; each compound shows the calculated mean average and respective SD, which is also included in each bar of the diagram.*

Interestingly, for the three samples of *1/P25/He/70°C*, which are illustrated in ***Figure 20***, the SD of both H_2 and CH_4 are slightly higher. To be precise, the SD of H_2 is larger by 0,5% and that of CH_4 by 4%. This may be due to the adjustment of three parameters, in comparison to *P25-Pt/He/RT/NM*. These parameter alterations entail the increase of temperature from RT to 70°C, the addition of PET as substrate and neat P25 as photocatalyst, rather than P25-Pt.
Although values in SD are greater than that of the previously discussed sample, and the SD of H_2 is close to 20%, it can hence be inferred that the applied methodology produces qualitatively reproducible outcome from repetition.

In addition to the reiterated samples, a 24 hour experiment of *1/P25/He/70°C*, illustrated in ***Figure 20***, was also performed, namely *1/P25/He/70°C/24h*. Hereby, the general procedure was indifferent, solely the irradiation period was augmented from 5 to 24 hours. For both experiments, the detection of the gaseous products took place before and after irradiation and no additional samples were measured. The results are displayed in ***Figure 21*** and ***22***. These figures depict the detected values in µmol, calculated from ppm, and additionally show the respective rates in µmol/h. The error bars included in the graphs, correlate with the values from the samples elaborated above, thus in µmol/h as well.

From ***Figure 21***, it can be concluded that over the course of 24 hours of irradiation, the rate of H_2 formation remains indifferent, respectively 0,029 µmol/h. In other words, approximately 5 times more H_2 was present, which equates well to the number of hours the experiment took place.
In contrast, a mere 22,9% of CH_4 remained measurable after 24 hours, whilst comparing to the 5 hour experiment, shown in ***Figure 22*** below. The exact cause for this is uncertain. Perhaps, generated CH_4 might have been consumed in the prolonged experimental period, yet the precise mechanism is uncharted and was not further explored during this work.
In summary, an extended irradiation period by the factor 4,8, concludes to roughly 5 times more H_2, but conversely this is not the case for CH_4. Here, a 93% decrease of the rate can be gathered from the acquired data, suggesting that CH_4 can be re-consumed (presumably oxidized) under prolonged reaction.

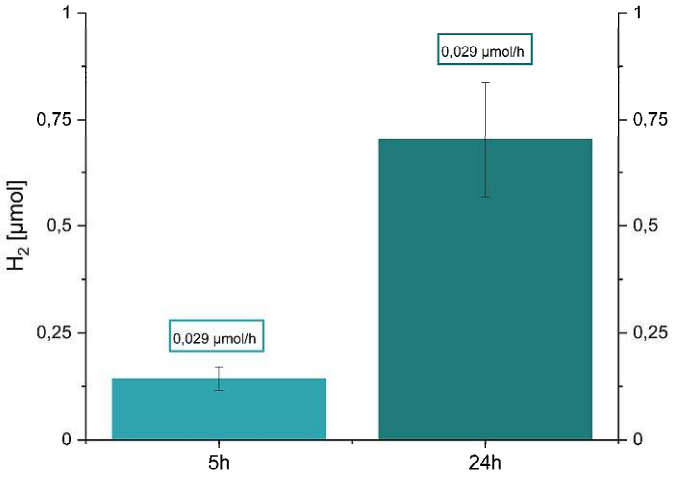

Figure 21: H_2 generation with P25 as photocatalyst and PET as substrate at 70°C; comparison of UV irradiation for 5 vs. 24 hours; image includes rate in µmol/h as well as measured values in µmol; SD ± 19,3%.

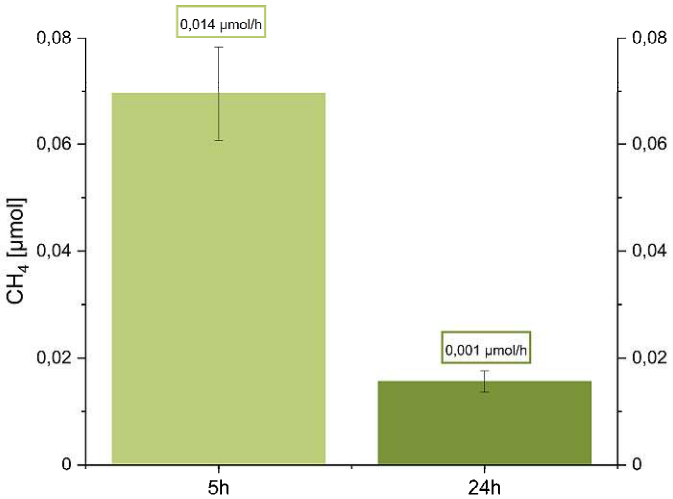

Figure 22: CH_4 generation with P25 as photocatalyst and PET as substrate at 70°C; comparison of UV irradiation for 5 vs. 24 hours; image includes rate in µmol/h as well as measured values in µmol; SD ± 12,7%.

5.3 Comparison of different substrates

After performing the set of measurements, discussed in the previous chapters, with PET (source 1) as substrate, it was of interest to conduct further investigations. Herein, PET from a second source was selected for comparability and the polyolefins PP and LDPE, as successful photoreforming of these microplastics is desirable to the scientific community.

Each substrate was dispersed in 1M NaOH, with P25-Pt as photocatalyst, and irradiated with a UV lamp for 5 hours, after purging with He for 10 minutes. The attained results are illustrated in ***Figure 23*** for H_2 and ***Figure 24*** in regards to CH_4.

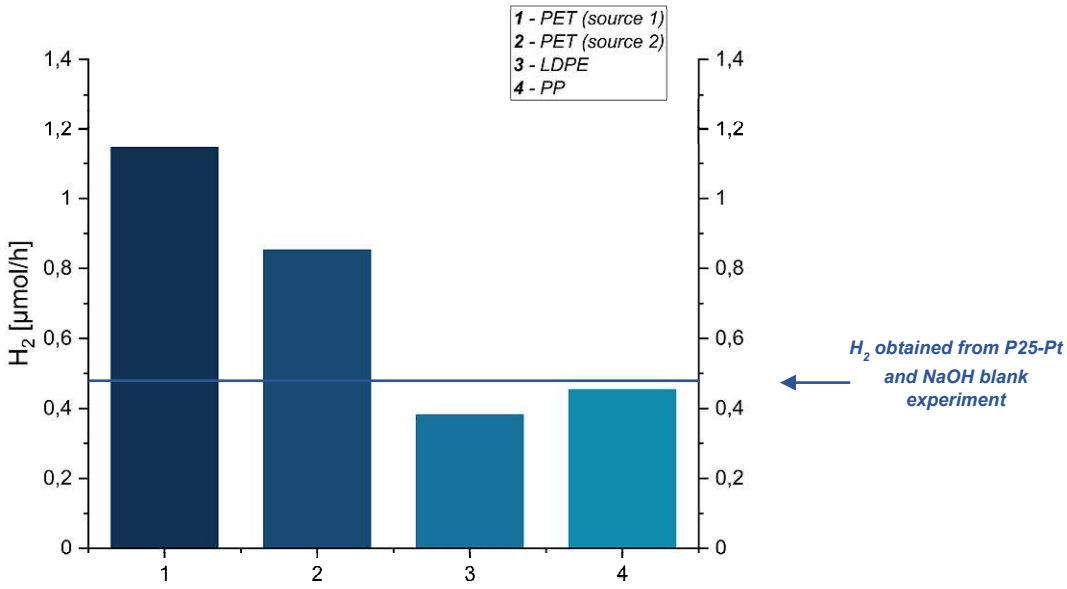

Figure 23: *H_2 formation from different substrates; experiments conducted under UV irradiation for 5 hours, in 1M NaOH, with P25-Pt as photocatalyst and at RT; 1 – 1/P25-Pt/He/RT; 2 – 2/P25-Pt/He/RT; 3 – 3/P25-Pt/He/RT and 4 – 4/P25-Pt/He/RT.*

The values in ***Figure 23*** show, that comparable results are achieved with PET from two different sources. The first source is a commercially obtained powdered microplastic. The second was a commercial PET, which was then ground by the collaborators providing us with the substrate. Therefore, it must be taken into consideration that the size distribution of the nanoparticles may vary here. Nevertheless, *2/P25-Pt/He/RT* achieved approximately 74% in value of H_2 formation in comparison to *1/P25-Pt/He/RT*. This is equivalent to 0,85 µmol/h. Conversely, the generation of H_2 from the respective microplastic, did not appear as successful in the case of LDPE and PP. The lower quantity of H_2 formed here, suggest that both of these studied substrates are rather "inactive" to the photoreforming process of this methodology. As both of these microplastics are comprised of a very stable C-C backbone and due to their hydrophobic nature, photoreforming is not as feasible as for plastics containing heteroatoms, such as N and O, in their backbone. In addition, these compounds do not entail any unsaturated chromophoric groups, thus light

absorption is impeded.[4,35] However, in contrast to sunlight, UV-irradiation is supposed to be sufficient for the initiation of bond cleavage of C-C or C-H bonds, as the wavelength of 365 nm coincides with the respective bond dissociation energies. The bond cleavage would in consequence form free radicals, promoting oxidation of the substrate.[34]

In the case of *3/P25-Pt/He/RT* a mere 0,38 µmol/h of H_2 were detected and for *4/P25-Pt/He/RT*, 0,45 µmol/h were measured. Both values are slightly below the 0,5 µmol/h generated with the sample, previously discussed, which solely contained the photocatalyst and no microplastic (*P25-Pt/He/RT/NM*). Thus it is believed that the values achieved for these two substrates, might be a consequence of direct water splitting of the water molecules present in the diluted NaOH solution, rather than due to the upcycling process of the microplastic under investigation.

Furthermore, whilst the procedure of PP was identical to PET, in terms of methodological flaws present, such as minor loss of liquid or photocatalyst when transferring the solution to the reaction vial, this was not the case for LDPE. In addition to the expected errors implemented in every experimental step, a majority of the substrate was floating on the surface of the solution, as it is rather lightweight. Moreover, when removing the needle of the gas line after purging, some of the substrate was sticking to it, thus adjusting the concentration of microplastic present in solution and further adding to the error of the procedure. Even whilst stirring the solution during the reaction, with a magnetic stirrer, it could not be guaranteed that the substrate was homogenously dispersed during irradiation, due to its lightweight and sticky nature. Although this most probably is not the sole cause of the minor values produced, it is necessary to take into consideration for possible future experiments.

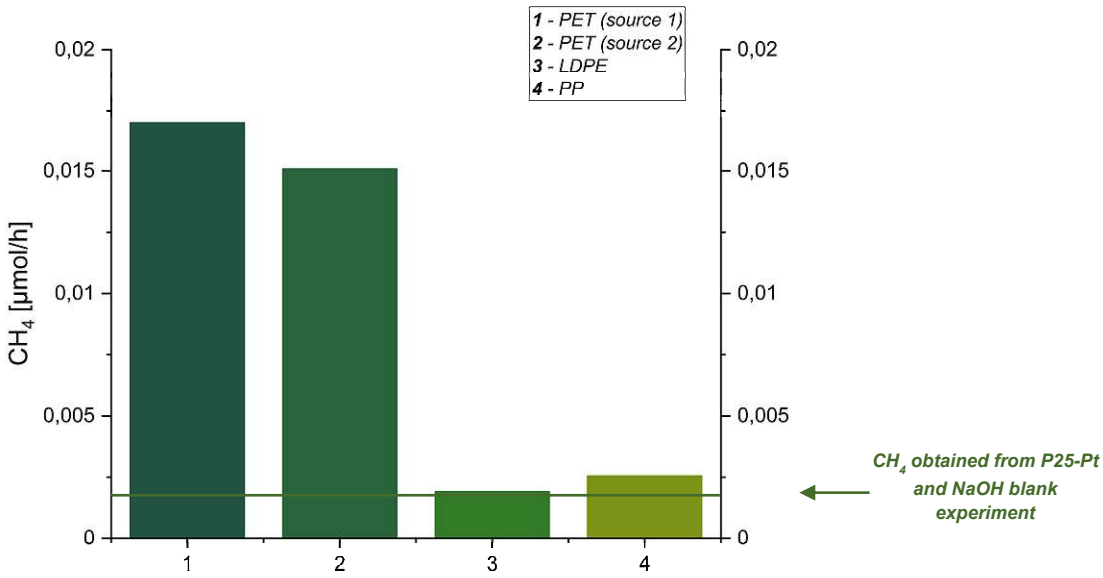

Figure 24: *CH_4 formation from different substrates; experiments conducted under UV irradiation for 5 hours, in 1M NaOH, with P25-Pt as photocatalyst and at RT; 1 – 1/P25-Pt/He/RT; 2 – 2/P25-Pt/He/RT; 3 – 3/P25-Pt/He/RT and 4 – 4/P25-Pt/He/RT.*

From ***Figure 24***, it can be gathered that the general trend is identical as was shown for H_2. The quantity obtained from both of the PET samples are again comparable, yet the difference in value is only around 12%, in contrast to the approximately 26% in the case of H_2 formation. As was the case above, the total of CH_4 achieved in the experiments containing LDPE or PP, are very close to the blank experiment, which did not incorporate a substrate. The respective values are 0,002 µmol/h for LDPE and 0,003 µmol/h for PP. Surprisingly, the quantity of PP amounts to the exact same value as for the discussed blank experiment. This is particularly peculiar, as it is believed that the CH_4 of the blank experiment may have originated from the PP cap. Therefore the question of origin of this compound remains.

Overall, as has been reported in literature, the most promising results are exhibited for the valorisation of PET. Consequently, the attention of this work was focused on the respective compound. Moreover, both PET sources display comparable results. This is of utmost importance, as the final aim of this subject would be the industrial application in plastic abasement and by no means are two plastic products completely identical. Therefore this demonstrates the feasibility for future approaches.

However, as aforementioned, plastics which are not solely comprised of C-C backbones, as is the case for polyolefins (for example PE and PP), would be better suited for the process. More favourable compounds include polycondensates, such as, nylon, PLA, PC and PUR, which (like PET) contain O or N in their backbone and are polar. This in consequence makes them more susceptible for hydrolytic cleavage into their respective monomers and thus can be upcycled more efficiently.[7,45]

Moreover, it is to be noted that the presence of PP in the solution did not appear to result in any addition of H_2 or CH_4, in contrast to the blank experiment *P25-Pt/He/RT/NM* discussed in a prior section.

5.4 Investigation of commercial applicability

In this section, experiments are being discussed, of which the aim was the study of future prospects in the industry. Herein, the influence of co-catalyst at room temperature (where the cost is increased by Pt) was put into contrast to neat P25 at elevated temperature (where the cost is increased by the need for external heating). As previously elaborated, a great aspiration in the field of photocatalysis is the opportunity on solely relying on the energy provided by the sun, to produce green fuels and simultaneously upcycle microplastics. The sun would present a highly effective and cheap source of energy. Although TiO_2 is UV active, it was of importance to investigate the possibility in applying a solar simulator, a Xe lamp with an IR-filter to be precise. In addition, a minimal upscaling of the setup was also executed, as this aspect as well provides knowledge on the feasibility of this method in a larger scale.

5.4.1 Experiments dedicated to solar simulation

The results presented here, were obtained whilst performing the same general procedure as previously illustrated, with the exception of reduction in volume of the solution, from 18 mL to 16mL, and the illumination with a Xe lamp, instead of a UV light source (***Table 4***, additional experiments, suffix “SS”). The concentration of both the photocatalyst and the substrate remained unchanged. The values depicted in ***Figure 25*** and ***26***, were measured after 24 hours of irradiation.

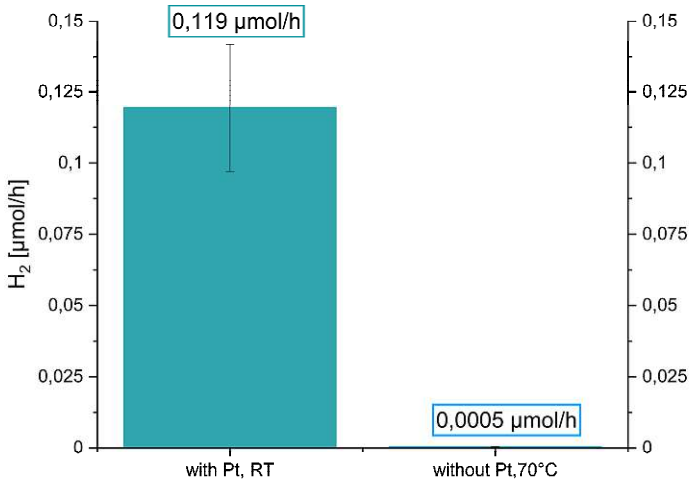

***Figure 25**: H_2 generation after 24 hours, “with Pt, RT” is 1/P25-Pt/He/RT/SS, showing a rate of 0,119 µmol/h and a SD ± 18,8%; “without Pt, 70°C” is 1/P25/He/70°C/SS, displaying a rate of 0,0005 µmol/h and SD ± 19,3%.*

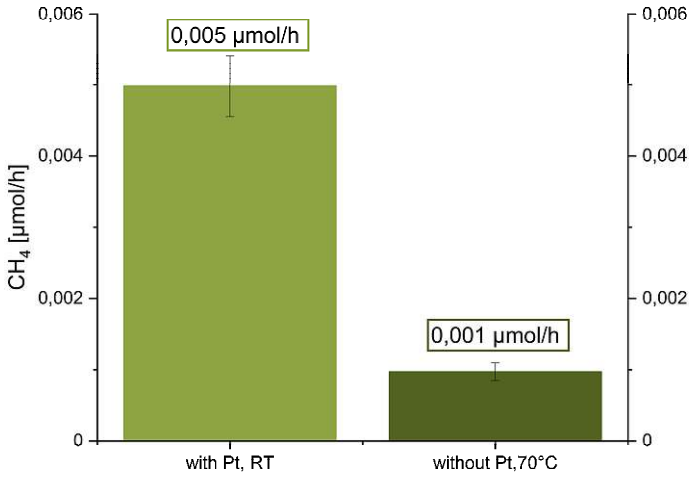

***Figure 26**: CH_4 generation after 24 hours, "with Pt, RT" is 1/P25-Pt/He/RT/SS, showing a rate of 0,005 µmol/h and a SD ± 8,7%; "without Pt, 70°C" is 1/P25/He/70°C/SS, displaying a rate of 0,001 µmol/h and SD ± 12,7%.*

As can be extracted from ***Figure 25***, a substantial amount of H_2 was produced under solar simulated light for the sample with Pt as co-catalyst, as compared to *1/P25/He/70°C/SS*. This further proves the advantageous impact that the presence of the noble metal has on water splitting. Overall, the rate of generated H_2 by *1/P25-Pt/He/RT/SS* equates to around 10,4% of the quantity achieved under UV irradiation with *1/P25-Pt/He/RT*, which commends this photosystem for the use under natural light. Conversely, *1/P25/He/RT/SS* underlines the necessity of a co-catalyst for successful H_2 production under solar illumination. Herein solely 1,7% in H_2 value was obtained at 70°C, in contrast to the sample irradiated with 365 nm. This corresponds to 0,0005 µmol/h in comparison to 0,029 µmol/h.

Regarding CH_4 evolution (***Figure 26***), the presence of the co-catalyst promotes the production of this gaseous product as well, with a rate of 0,005 µmol/h compared to the 0,017 µmol/h attained with the UV lamp. In other words, this represents approximately 29,4%, again suggesting applicability of this photocatalyst under solar light. The data acquired at 70°C, demonstrate a rate of 0,001 µmol/h for the production of CH_4, complying with 7% of the respective sample irradiated with a UV light source. Moreover, ***Figure 26*** clearly demonstrates the advantageous influence of the co-catalyst on the photoreforming process, as 5 times more CH_4 was produced in contrast to the sample irradiated at 70°C. This emphasizes, the employment of a co-catalyst to be considered for commercial application, as the price-performance ratio would be more reasonable.

The two samples portrayed here, demonstrate the possibility in utilizing the sun for the generation of the presented solar fuels. This being said, the data further underlines the necessity of a co-catalyst, if TiO_2 is desired as photocatalyst. Interestingly both reviewed data sets suggest that, with the Xe lamp, more CH_4 was formed than H_2. The opposite was the case for the respective samples under UV illumination. The reason for this is yet to be studied.

5.4.2 Investigation of an upscaled setup

The two samples of interest within this chapter, were conducted in an upscaled manner (***Table 4***, additional experiments, suffix "UP") This involved an increase in volume to 100 mL and an extended irradiation period of 32 hours.

The results obtained for H_2, are summarized in ***Figure 27a*** and ***27b*** for *1/P25-Pt/He/RT/UP* and in ***Figure 29a*** and ***29b*** for *1/P25/He/70°C/UP*. The same is illustrated for CH_4 in ***Figure 28a*** and ***28b*** for the room temperature experiment and in ***Figure 30a*** and ***30b*** for the sample irradiated at 70°C.

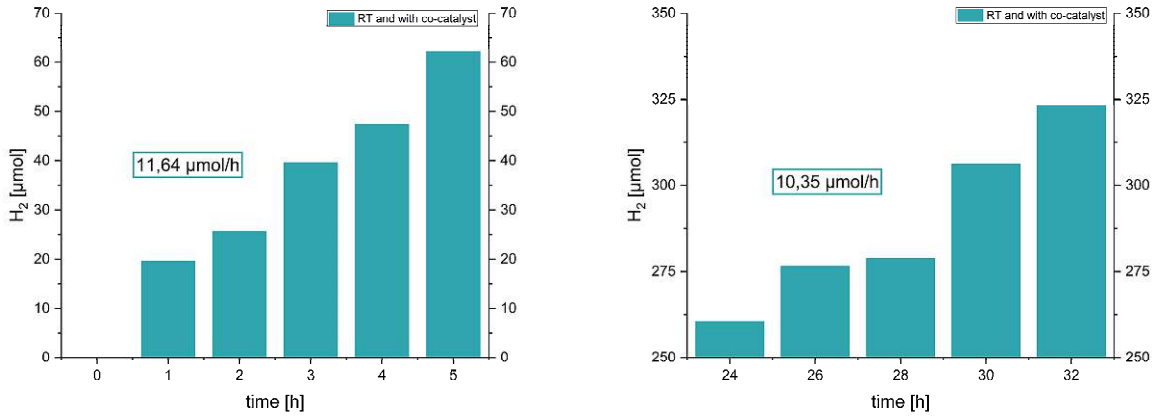

***Figure 27**: H_2 generation of 1/P25-Pt/He/RT/UP in a span of 32 hours and upscaled setup, measured values presented in µmol; **27a** (left) shows the data from hour 0 – 5 with a rate of 11,64 µmol/h, **27b** (right) depicts hour 24 – 32 with a rate of 10,35 µmol/h.*

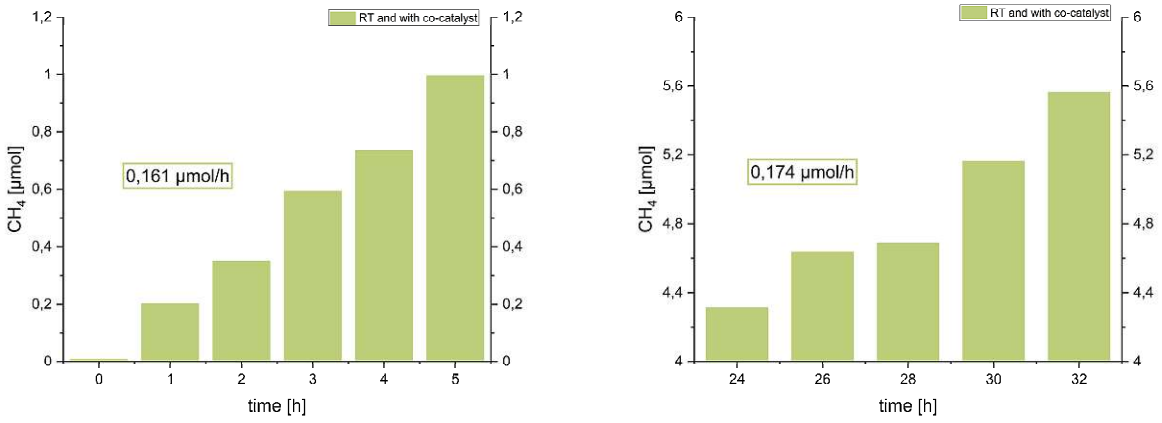

***Figure 28**: CH_4 generation of 1/P25-Pt/He/RT/UP in a span of 32 hours and upscaled setup, measured values presented in µmol; **28a** (left) shows the data from hour 0 – 5 with a rate of 0,161 µmol/h, **28b** (right) depicts hour 24 – 32 with a rate of 0,174 µmol/h.*

In ***Figure 27a***, a steady accumulation of H_2 can be deduced within the first 5 hours of the experiment, comprised of P25-Pt and conducted at RT. The rate of H_2 generation here is 11,64 µmol/h. Between hour 24 and 32, presented in ***Figure 27b***, the H_2 production is still present, yet a minor deactivation of the photocatalyst can be recognised, as the production rate diminished to 10,35 µmol/h. In comparison to the lab scale experiment, the enlarged system (by a factor of around 5 in terms of volume), has consequently yielded 11 times more H_2 within the first 5 hours. In regards to CH_4, the same trend can be observed. Within the first 5 hours, demonstrated in ***Figure 28a***, there is a constant generation of CH_4 with a rate of 0,161 µmol/h. Moreover, the 0,995 µmol generated after 5 hours, is again 11 times more than the produced 0,085 µmol achieved with the lab scaled experiment. Whilst comparing the calculated rates in ***Figure 28a*** and ***28b***, an acceleration of photocatalyst activity can be concluded, with an increase by around 8%.This corresponds to a rise by 0,013 µmol/h. When comparing both graphs in ***Figure 28***, of the upscaled RT experiment with Pt, to the results of *1/P25/He/70°C*, setting 5 hours of irradiation in contrast to 24 hours (***Figure 22***) the long-term stability of the photocatalyst can be evaluated. As aforementioned, the former demonstrates an acceleration in photocatalyst activity regarding CH_4 production. In contrast, the latter shows 14 times less CH_4 produced after 24 hours in comparison to the detected value after 5 hours. This indicates the impact of temperature on the photocatalyst stability. Whilst the photocatalyst appears stable even after 32 hours for *1/P25-Pt/He/RT/UP*, this is shown not be the case for the experiment with exalted temperature and in a lab scale. In other words, a "high" temperature of 70°C appears detrimental to the stability of the photocatalyst and reducing the selectivity towards CH_4 formation, whilst a "low" temperature, i.e. RT, enhances its stability and subsequently aids its long-term performance.

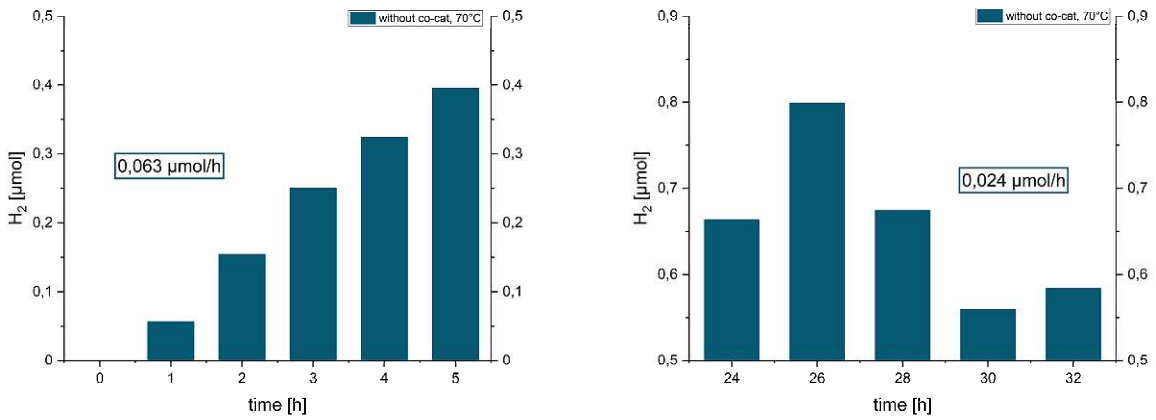

Figure 29: *H_2 generation of 1/P25/He/70°C/UP in a span of 32 hours and upscaled setup, measured values presented in µmol;* ***29a*** *(left) shows the data from hour 0 – 5 with a rate of 0,063 µmol/h,* ***29b*** *(right) depicts hour 24 – 32 with a rate of 0,024 µmol/h.*

The H_2 production of the upscaled experiment comprised of neat P25 and 70°C is summarized in ***Figure 29a*** for hour 0-5 and in ***Figure 29b*** for hour 24-32. Within the first 5 hours of the experiment, similar to the sample discussed above, there is an addition of H_2 within every hour, with a rate of 0,063 µmol/h. In comparison to *1/P25-Pt/He/RT/UP*, a mere 0,079 µmol/h were generated after 5 hours, as to the 12,43 µmol/h obtained with the presence of the co-catalyst. Furthermore, this equates to only 55% of the amount generated in the small-scaled setup Between the hours 24 and 32, no particular trend can be recognized. A large jump is present between 24 and 26, but the values decrease afterwards before there is a slight elevation again between 30 and 32. Hence, the rate of 0,024 µmol/h is not entirely credible.

The presence of a temperature gradient may have been the cause of these results. As aforementioned, no oil bath was employed as there was no guarantee that the UV light would then sufficiently irradiate the sample. In addition, the exact temperature within the solution was unknown, as no thermometer was used, due to the necessity of the system being closed, and the settings of the heating plate were taken from preliminary evaluation for the glass vial experiments. Although the solution was stirred and thus promoting certain homogeneity, it is not impossible that the actual temperature value was below 70°C. Therefore, the results attained for this experiment are not fully reliable.

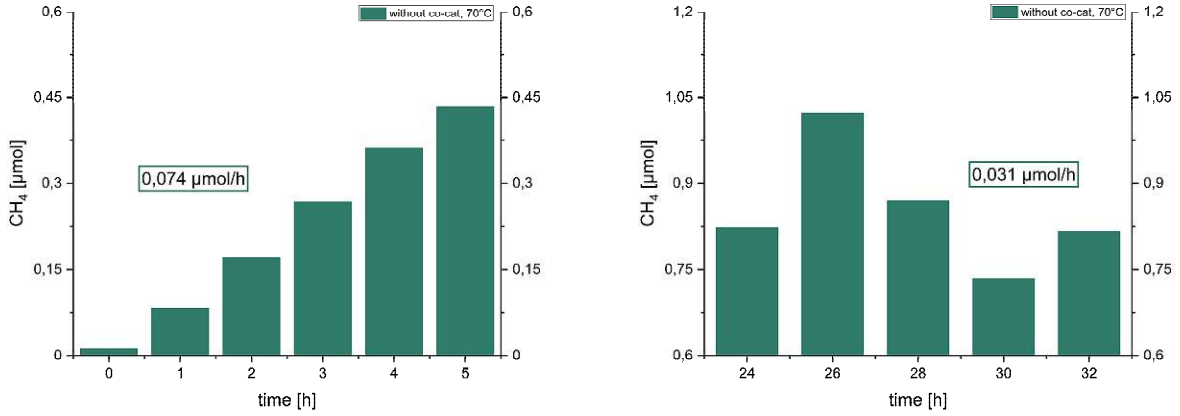

Figure 30: *CH_4 generation of 1/P25/He/70°C/UP in a span of 32 hours and upscaled setup, measured values presented in µmol*; ***30a*** *(left) shows the data from hour 0 – 5 with a rate of 0,074 µmol/h,* ***30b*** *(right) depicts hour 24 – 32 with a rate of 0,031 µmol/h.*

The data acquired for CH_4 provides similar results to H_2, as is demonstrated in ***Figure 30a*** for hour 0 – 5 and in ***Figure 30b*** for hour 24 – 32. The rate of CH_4 generation appears to be minorly greater than for H_2, with a value of 0,074 µmol/h, within the first 5 hours. In regards to the second day of the experiment, anew several fluctuations are visible, thus the rate of 0,031 µmol/h is not plausible. Conversely to the reiterated experiment, elaborated in *chapter 5.2.3*, *1/P25/He/70°C/UP* exhibits a higher value in CH_4 production compared to H_2, after 5 hours. This equates to an increase by around 10%. Even after 32 hours, it appears as though a greater

quantity of CH_4 has been generated than H_2. As the mechanism of the process is yet to be established, the reason for this is unknown.

Overall, the most promising outcome can be concluded from the sample with Pt as co-catalyst. Herein, the production of both gases, in µmol generated per mg photocatalyst, doubled in comparison to the small batch experiment. This equates to 1,24 µmol/mg in H_2 and 0,02 µmol/mg in CH_4. Conversely, a diminished value for H_2 was achieved for irradiation at exalted temperature and with neat P25, with a value of 0,008 µmol/mg. In contrast, the respective lab scale experiment produced 0,016 µmol/mg in H_2. However, an increase of CH_4 by 29% (0,009 µmol/mg) can be inferred from the obtained data of the upscaled setup. This suggests that the presence of the temperature gradient and thus slightly lower temperature aids the generation of CH_4 in an upscaled manner. This in consequence demonstrates that there might be an ideal temperature for the photocatalyst stability and performance. In other words, high temperature is more selective towards H_2 formation and a temperature slightly below 70°C promotes the generation of CH_4. Nonetheless, low temperatures (RT) and the presence of Pt provide the most promising results for an industrial environment.

The aforementioned values again emphasize the beneficial impact achieved by the implementation of a co-catalyst in respect to both water splitting and the oxidation of the microplastic, fostering the H_2 and CH_4 synthesis. In contrast, neat P25 combined with elevated temperature does not appear to result in sufficient generation of either gas. However, it must be considered that a better-established procedure, where temperature can efficiently be controlled, might yet yield more favourable results.

5.5 Analysis of upcycled products

Finally, the upcycling products, of some of the previously discussed samples, were analysed via HPLC, with H_3PO_4 as eluent. Herein, the focus was set on the four preliminary samples purged with CA (experiment A, B, E and F from main series in ***Table 4***), the two upscaled (additional experiments C and H with suffix "UP" in ***Table 4***) and solar simulated samples (additional experiments C and H with suffix "SS" ***Table 4***) and the 24 hours experiment (additional experiment H with suffix 24h in ***Table 4***). In addition, *1/P25-Pt/He/70°C* (experiment G from main series in ***Table 4***) was also measured, as it demonstrated the advantageous influence of both temperature and co-catalyst to the photoreforming method. In general, all filtered solutions were transparent, with the exception of *1/P25-Pt/He/70°C* and *1/P25-Pt/He/RT/UP*, which occurred pale yellow. The most outstanding outcome for H_2 and CH_4 generation were obtained for these two samples, respectively.

In numerous works published by *Uekert et al.*, some of the expected products, from photocatalytic upcycling of PET, included for example terephthalic acid, formate, acetate, ethanol and glycolic acid. To be precise in one of their studies, ethylene glycol was the substrate under investigation, as it is a monomer of PET. Herein, they were able to assess glyoxal, glycoaldehyde, glycolate, glyoxylate, formate and carbonate as oxidation products.[44,46,50]

In the course of this work, standard solutions of formic acid (FA), acetic acid (AA), oxalic acid (OA) and ethylene glycol (EG) were prepared and measured. All standard solutions were clear in colour. The respective calibration equations and retention times are illustrated in ***Table 5***.

Table 5*: Overview of retention times and obtained equations of selected standards.*

Compound	Retention time [min]	Equation
FA	11,308	y = 34235.6x
OA	6,822	y = 51674.0x
AA	11,98	y = 50541.7x
EG	12,958	y = 74720.4x

Upon analysis, no FA could be concluded for any of the samples measured. The following table, ***Table 6***, summarizes the acquired high-value chemicals for each analysed sample. Furthermore, ***Figure 31*** depicts the chemical structure of PET and the obtained photoreforming products. It can be concluded from the image, that both OA and EG represent C_2 structures, i.e. comprised of two C-atoms. In contrast, AA only constitutes of a single C-atom and thus is the most oxidized compound out of the three. The obtained results are presented in ***Figure 32***.

***Table 6**: Synopsis of detected products in the respective analysed sample.*

Experiment number	Sample	Products found
A	1/P25-Pt/CA/RT	OA
B	1/P25/CA/RT	OA
E	1/P25-Pt/CA/70°C	OA, AA
F	1/P25/CA/70°C	AA, EG
G	1/P25-Pt/He/70°C	AA, EG
C	1/P25-Pt/He/RT/UP	OA, AA
C	1/P25-Pt/He/RT/SS	AA
H	1/P25/He/70°C/24h	AA, EG
H	1/P25/He/70°C/UP	AA, EG
H	1/P25/He/70°C/SS	EG

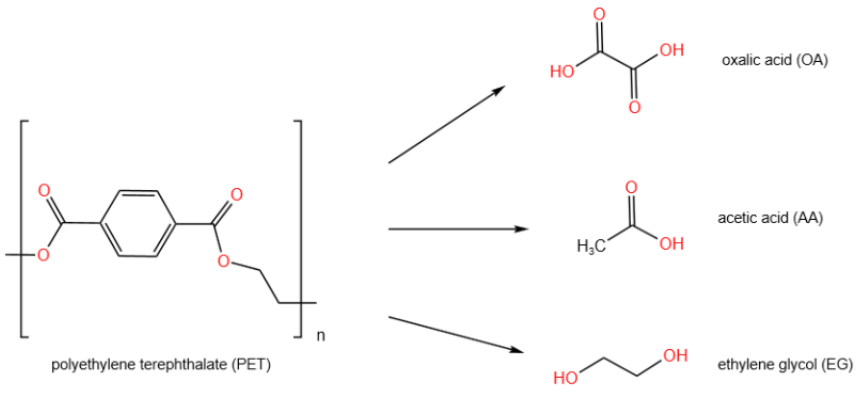

***Figure 31**: Chemical structure of the investigated substrate PET (left) and the consequently formed photoreforming products OA, AA and EG (right).*

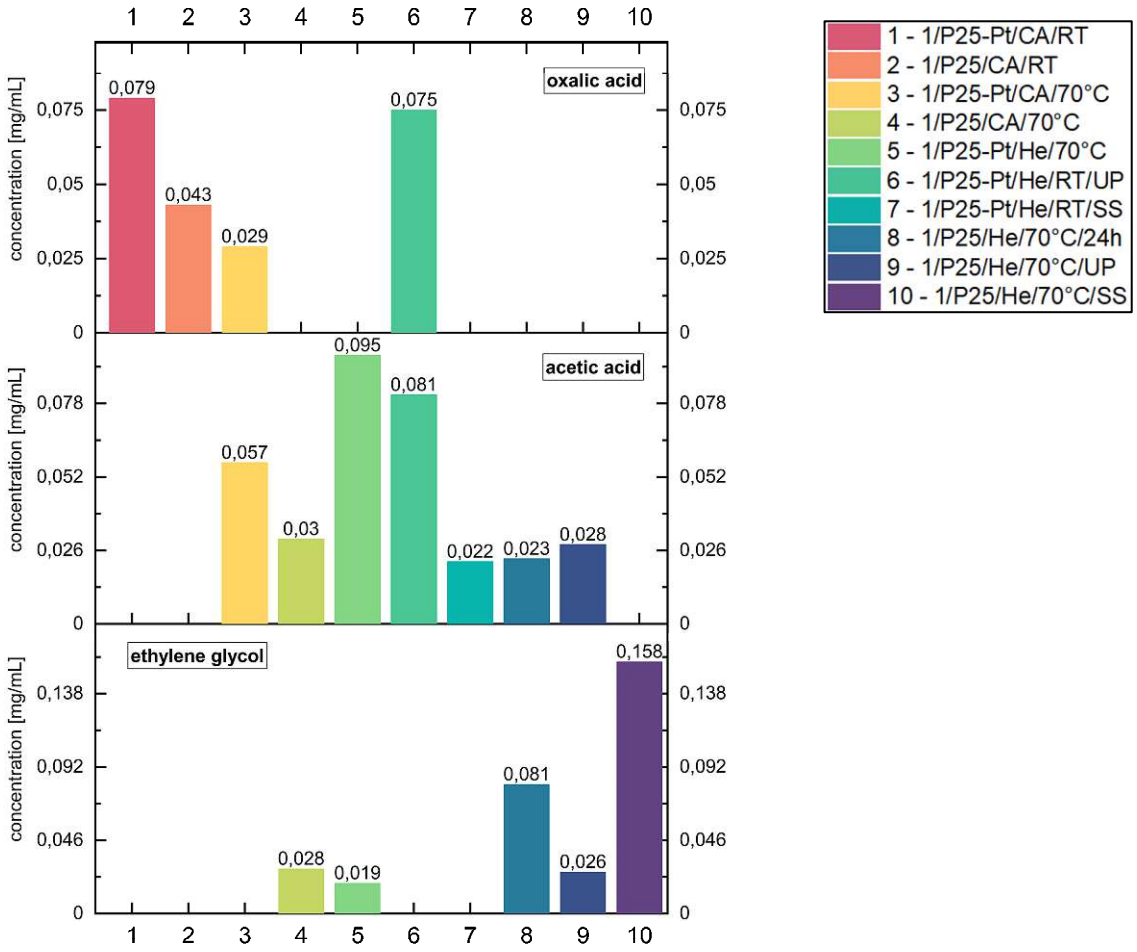

Figure 32: *Result from the HPLC measurements, top: samples presenting oxalic acid (OA), middle: samples containing acetic acid (AA), bottom: samples comprised of ethylene glycol (EG).*

From ***Figure 32*** *(top)* it can be gathered that three out of the four analysed CA samples contain OA, with the highest concentration obtained for the sample with Pt and irradiated at RT. Interestingly, *1/P25/CA/70°C* does not exhibit any OA, although the application of temperature is believed to aid substrate hydrolysis, as was elaborated in previous chapters. Additionally, *1/P25-Pt/He/RT/UP* of the upscaled experiment, yields the second highest concentration of OA for the analysed series of samples, with a value of 0,075 mg/mL. In other words, around 7,5% of the initial 1 mg/mL of PET was oxidized to OA.

In regards to AA (***Figure 32,*** *middle*), both samples, of which the solution exhibited a pale yellow colour, yielded the highest concentration of this compound. The sample comprised of Pt co-catalyst and irradiated at elevated temperature, *1/P25-Pt/He/70°C*, contains 0,095 mg/mL of AA, thus 9,5% of PET was formed into this chemical. The two following highest values were obtained for both CA samples, which were illuminated at 70°C. Although, *1/P25-Pt/CA/70°C* concluded in a mere 60% of the concentration achieved under inert conditions, this accentuates the requirement of temperature for the formation of AA, when purging with CA. The lowest

concentrations were measured for *1/P25-Pt/He/RT/SS* and *1/P25/He/70°C/24h*. For the former, AA is the only product found so far. As there is no comparison to the sample irradiated with UV light source, no tangible claims can be made. The latter, combined with *1/P25/He/70°C/UP*, emphasizes the necessity in taking temperature into consideration if the application of neat P25 is desired.

The results for EG, shown in ***Figure 32*** *(bottom)*, entail the highest product concentration among all samples measured. This is demonstrated by *1/P25/He/70°C/SS* with a value of 0,158 mg/mL. This result appears to be counterintuitive, as the experiment was conducted with the Xe-lamp and neat P25. Overall, the largest yields of EG were achieved for the experiments comprised of P25, irradiated at 70°C and purged with He. A minor decrease can be extracted for the upscaled experiment, which could be a result of a temperature gradient, as described in the previous chapter. The smallest quantity of EG was detected for *1/P25-Pt/He/70°C* which is the only sample with co-catalyst, that presents this product. All of the samples presented here were obtained from inert conditions, with the exception of *1/P25/CA/70°C*, which displays a concentration of 0,028 mg/mL.

From literature it can be extracted that EG is primarily formed by hydrolysis of PET in the strong alkaline media. Another expected monomer would be terephthalic acid, which, as aforementioned, was not included in the HPLC measurements. The proposed mechanism is as follows (***Figure 33*** and ***34***): the photogenerated h^+ oxidize EG to glycolaldehyde, which then produces glycolate and glyoxal via radicals. Both of these compounds subsequently produce glyoxylate, which then results in oxalate. This would then form formate, which finally results in carbonate. Furthermore, it has been reported that EG can also produce ethanol in the case of hydrodeoxygenation, which subsequently can oxidize to acetaldehyde and acetic acid.[30,46]

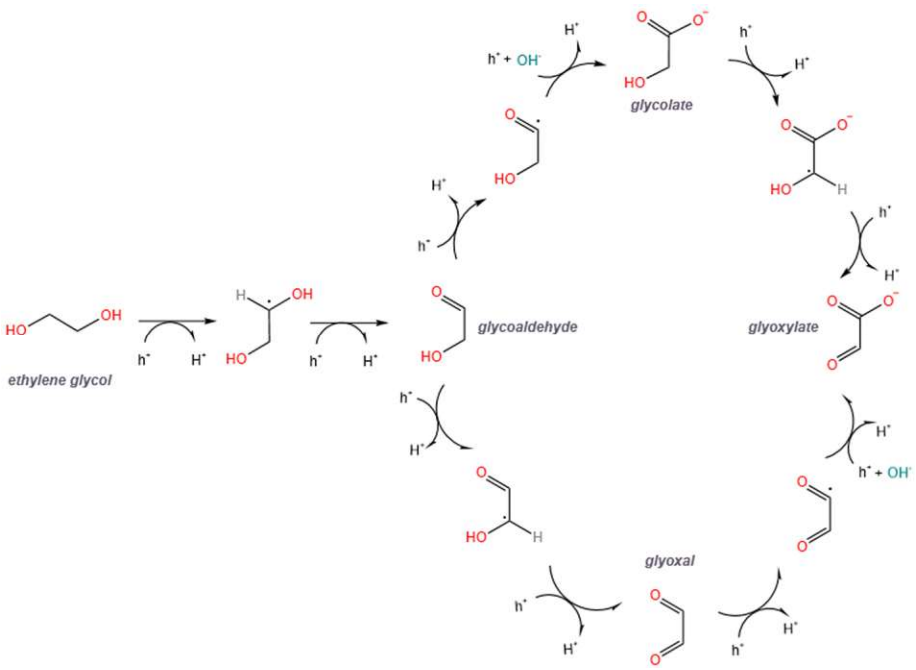

Figure 33*: First half of the oxidation mechanism of EG to glycoaldehyde and subsequently to glyoxylate, as suggested by Uekert et al.*[46]

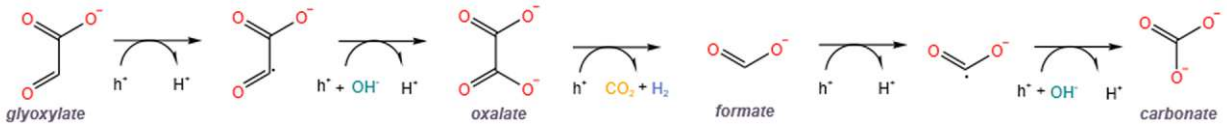

***Figure 34**: Second half of the oxidation mechanism of EG, from glyoxylate to carbonate, as suggested by Uekert et al.*[46]

This can also be concluded from the presented results, as primarily samples obtained from inert conditions show AA. However, the two CA samples, which were collected from experiments at exalted temperature, also contain AA. This gives to believe that the presence of temperature might in addition have an impact on the formation of this compound. Moreover, whilst comparing the results obtained for both OA and EG, it can be gathered that samples containing the former, did not display the latter. Therefore, a possibility could be that all of the EG produced via hydrolysis during photoreforming, converted to OA. However, it is unclear why no formic acid could be detected. Regarding EG, the two highest values could be concluded for *1/P25/He/70°C/24h* and *1/P25/He/70°C/SS*. These samples are indifferent in terms of temperature, photocatalyst and substrate. Nonetheless, an adjustment in light source, from UV to solar spectrum, appears to have aided the formation of EG substantially. Overall, it can be concluded that the enhancement of temperature can promote generation of EG.

In summary, there is no apparent advantage of CA to He, regarding the number of products formed or their concentration. It can merely be stated, that the majority of samples which contain OA were in fact purged with CA and the highest yield for upcycling from PET, was demonstrated for samples showing EG as product, with approximately 16% in conversion. Furthermore, no clear influence of temperature nor photocatalyst can be evaluated from the received data. However, it needs to be taken into consideration that solely four compounds from a long list of expected products were investigated. A more thorough study, with a greater set of samples and standard solutions for example, would be required to make further deductions.

6. Conclusion

In summary, the concepts of photoreforming were proven, as is illustrated in ***Figure 14a*** and ***14b***. Further, it could be concluded that around 0,499 µmol/h in H_2 and 0,003 µmol/h in CH_4 were obtained from the sample solely comprised of photocatalyst and NaOH.

An experimental set, which investigated various parameters, under inert atmosphere and with PET as substrate, showed that the highest values in both H_2 and CH_4 were achieved with the samples comprised of P25-Pt, namely ***1***/*P25-Pt/He/RT* and ***1***/*P25-Pt/He/70°C*. This is an indicator for the beneficial impact of employing a co-catalyst, in regards to solar fuel generation. Moreover, the latter exhibited approximately 24% more H_2 and 5 times more CH_4, thus demonstrating the advantageous influence of exalted temperature on the degradation of the substrate, as was previously reported by *Nagakawa and Nagata*.[47] Upon gravimetric analysis, experiments conducted with He concluded in the highest degrees of degradation, demonstrating that oxidation predominantly takes places via direct h^+ transfer.

Once the methodology was established, it was of interest to investigate the reproducibility of received data. Hereby, two sets of examples, *P25-Pt/He/RT/NM* and ***1***/*P25/He/70°C*, were studied, each reiterated three times. This resulted in qualitatively comparable data. In addition, an experiment with a prolonged irradiation of 24 hours, with neat P25, at 70°C and PET as substrate, was performed as well. Although, roughly 5 times more H_2 was generated as a result of increasing the irradiation period by the same factor, this was not the case for CH_4. Conversely, the rate in CH_4 formation decreased by 93%. The cause for this is unknown, but the consumption of some of the generated CH_4, during the reaction period, is a possibility which needs to be taken into consideration. Furthermore, photoreforming of additional substrates, with the established methodology, was further investigated. From this it could be deduced that both PP and LDPE are rather “inactive” with the implemented setup, due to their very stable C-C backbone.

With future commercial application in mind, the two experiments, ***1***/*P25-Pt/He/RT* and ***1***/*P25/He/70°C*, were conducted with a Xe lamp, as solar simulator, and in an upscaled manner as well. The data obtained from the former, emphasizes the requirement of a co-catalyst for P25 to be photocatalytically active in the visible range. In addition, both samples generated more CH_4 in contrast to H_2, which is the opposite result to UV irradiation. Regarding the latter, promising values were attained from the sample with Pt and irradiation at RT. This again, underlines the great outcome achievable in the presence of a co-catalyst. In contrast, the sample of neat P25 and 70°C, exhibited lower values and fluctuations in rate between hour 24 and 32, for both gaseous products. This could be a consequence of a temperature gradient, induced by the insufficient setup.

Finally, OA, AA and EG were detected in selected samples. As previously mentioned, EG, one of the main hydrolysis products of PET, was measured mainly for samples irradiated at elevated temperatures. Further, it could be concluded that, samples which demonstrated OA, did not contain EG. This suggests a direct conversion from the latter to the former, during the photoreforming process. Notably, samples demonstrating AA were primarily obtained from experiments with an inert atmosphere. It is suggested that this is a result of a hydrodeoxygenation of EG to ethanol and in consequence to the investigated compound, i.e. AA.

Overall, both exalted temperature and co-catalyst are believed to aid the photoreforming process, but the results of this work suggest that the latter does more so.

7. Future outlook

This work aimed on establishing a methodology for the study of various parameters and the impact they have on the photoreforming process. Whilst a majority of this study relied on PET as substrate and solely a short investigation was conducted on PP and LDPE, broadening the spectrum of substrates to PLA for example, might be of interest. Several previous publications, as elucidated above, were able to report success in the upcycling of this biodegradable microplastic. However, hitherto the focus was aimed at H_2 generation and no data has been described in regards to CH_4. Once results have been acquired for other plastics, performing long-term experiments of the microplastics in comparison to cut-outs of everyday objects comprised of the respective material, could provide further insight in the application in an industrial scale. This would be of significance, as many objects comprised of synthetic macromolecules, contain a number of additives, such as stabilizers, pigments, antioxidants and flame retardants, to prolong their durability.[7]

Moreover, a thorough study on the mechanism of the process would be of utmost importance as the exact origin of generated CH_4 has not been explored thus far. This would involve a more precise research on possible reactions of PET, which produce the respective gas. Furthermore, employing different characterisation methods, for example thermogravimetric analysis (TGA), to investigate the occurrence of phase transitions, or performing in situ diffuse reflectance IR Fourier transform spectroscopy studies (DRIFTS), could provide a better understanding of the underlying reduction mechanism.

Regarding examination of formed upcycling products in the liquid phase, measuring further standard solution of expected oxidation products from PET, such as terephthalic acid or ethanol, could provide further knowledge. In addition, this could also be essential to the elucidation of the present mechanism and its dependency on the studied parameters. Working with other methodologies in the analysis of the liquid phase, such as attenuated total reflection infrared spectroscopy (ATR-IR), could offer further conclusive results regarding products that are present and the mechanism of their formation.

Finally, as TiO_2 is an inexpensive and among the most effective photocatalysts in terms of water splitting, as of yet, and the addition of a co-catalyst has proven to be necessary to obtain promising results, continuing the presented study with other co-catalysts could be of value. Although Pt has often shown to be very advantageous to the generation of H_2, the scientific community is attempting to acquire cheaper and more abundant alternatives, such as Cu or Mn.[61,62] Moreover, studying the effect of isolation strategy and the effect of various loadings could be of interest as well.[63] As both of these strategies have been thoroughly studied in the aspect of photocatalytic water splitting, exploring these in the photoreforming of PET might be beneficial.

8. Appendix

8.1 A brief history on photoreforming

The presented table, ***Table 7***, offers a broad overview of the history of state of the art photocatalysts applied in the photocatalytic conversion of polymers and natural macromolecules. This summary entails, type of photocatalyst (PC), investigated substrate, reaction medium (RM), co-catalyst, gaseous products (P_g), high-value products in solution ($P_{l)}$, year of publication and reference.

***Table 7**: Summary of some of the reported photocatalysts studied in the application of photoreforming.*

PC	Substrate	RM	Co-catalyst	P_g	P_l	Year	Reference
$RuO_2/TiO_2/Pt$	Sugar, starch, cellulose	**sugar & starch:** H_2O **cellulose:** 6M NaOH or H_2O	Pt	H_2 & CO_2 small amounts of CH_3OH & C_2H_5OH	X	1980	**Kawai & Sakata** https://doi.org/10.1038/286474a0
TiO_2/Pt	**CI:** PVC, trichlobenzene, trichlorethylene **N:** amino acids, protein (MW=10,000-70,000), dead cockroaches, green algae (chlorella), animal excrement **other:** teflon, PVAL, PE	H_2O or 5M NaOH	Pt	H_2 and CO_2	HCl and NH_3	1981	**Kawai & Sakata** https://doi.org/10.1246/cl.1981.81
CdS/CdO_x QDs	lignocellulose, hemicellulose, cellulose, lignin	deaerated aqu. solution or 10M KOH	Co	H_2	**cellulose:** smaller saccharides formed	2017	**Wakerly et al.** https://doi.org/10.1038/nenergy.2017.21
CdS/CdO_x QDs	PLA. PET, PUR (also investigated PMMA,LDPE,PS,PVP, PEG, PVC, PC, but unsuccessfully)	NaOH	X	H_2	**PET:** acetate/formate/glycolate/lactate **PLA**: pyruvat/ alkalinity-induced pyruvat-based compound **PUR:** formate, acetate, pyruvate, lactate	2018	**Uekert et al.** https://doi.org/10.1039/C8EE01408F
$^{NCN}CN_x$	lignocellulosic biomass (α-cellulose, cellobiose, glucose, xylan, xylose, galactose, lignin, sinapyl alcohol)	aqu. KP_i + 4-MBA	NiP (Ni bis(diphosphine)), heterogeneous Pt, MoS_2	H_2 & negligible amount of CO and CO_2	formate, carboxylic groups of lower molecular weight polysaccharides	2018	**Kasap et al.** https://doi.org/10.1021/jacs.8b07853
CN_x/Ni_2P (cyanmaid functionalized)	PET and PLA (but also (LD)PE, PUR, PP, PS-block-polybutadiene)	1M KOH	2wt% Ni_2P	H_2	(after 5 days) **PET:** acetate/formate/glycolate/glyoxal **PLA**: acetate/formate, CO_3^{2-}	2019	**Uekert et al.** https://doi.org/10.1021/jacs.9b06872
homoegenous CDs	**insoluable biomass**: α-cellulose, lignin, xylan **industrially relevant**: EtOH,glycerol	purified H_2O; aqu. KP_i (pH6, 25°C); KOH 10M (pH15); H_2SO_4 (pH 2)	NiP (Ni bis(diphosphine))	H_2	**α-cellulose:** $C_6H_{12}O_6$ and $C_6H_{10}O_3$	2020	**Achilleos et al.** https://doi.org/10.1002/anie.202008217
CN_x/Ni_2P	cellulose, PET, municipal solid waste (and PLA)	H_2O or 0,5M KOH	2wt% Ni_2P	H_2	**EG** (monomer of PET): glycoaldhyde, glyoxal, glycolate, glyoxlate, formate, carbonate **α-cellulose:** formate	2020	**Uekert et al.** https://doi.org/10.1002/cssc.202002580
$CdO_x/CdS/SiC$	α-cellulose, lignin, albumin (from egg), keratin, PE,isoprene rubber	10M NaOH	Pt	H_2, CO_2 (here: final product of PR)	hydrolysis intermediates of cellulose: low-molecular weight polysaccharides, monosacchsarides, HMFs, organic acids	2021	**Nagakawa & Nagata** https://doi.org/10.1021/acsami.1c11888
TiO_2-$Co(terpyridine)_2$	cellulose	MeCN:H_2O (2:1)	CotpyP (= Co(II) bearing two 4'-phosphonated 2,2':6'2"-terpyridinie ligands with BF_4^- as counter anions)	CO, H_2	arabinose + formate	2021	**Lam & Reisner** https://doi.org/10.1002/anie.202108492
CdS nanorods, tipped with MoS_2	PET, PLA, PE	~60mL supernatant substrate solution (from pre-treatment = alkaline conditions)	X	H_2 gaseous alkanes (methane, ethane, propane, n-pentane)	**PLA:** Co_3^{2-}formate **PET**: formate, acetate, glycolate,Co_3^{2-} **PE:** methane, ethane, propane, n-pentane	2022	**Du et al.** https://doi.org/10.1021/acscatal.2c03605
carbonized polymer dots-graphitic carbon nitirde (CPDs-CN)	**PET** (drink bottles) **PLA** (packaging bags) (cut into small pieces, washed, dried, then pre-treated)	1M KOH (photocatalyst and substrate directly dispersed in it and sonicated)	Pt	H_2 (**PET** and **PLA**) CO_2 (**PLA**)	**PET:** glycolic acid, glycoaldehyde EtOH, high purity terephthalic acid	2022	**Han et al.** https://doi.org/10.1016/j.apcatb.2022.121662

CN_x (deposited on LD hollow glass microspheres = HGM)	cellulose, PET, turbid waste	1M KOH (with EG and substrate)	Pt vs Ni_2P	H_2	X	2022	**Linley & Reisner** 10.26434/chemrxiv-2022-t0jzc
TiO_2-Cu (different Cu species on P25)	cellulose (ball milled, 3:1 weight ratio agate balls:cellulose, 500rpm, 7h, reversing rotary every 60 mins, with 1 min pause)	water	Cu species	H_2 and CO_2	X	2022	**Belda-Marco et al.** https://doi.org/10.1016/j.cattod.2022.11.006
CuO or CuO_2 on TiO_2 (P25)	glycerol	substrate = solution (catalyst drop casted onto Cu grids and added to the glycerol solution)	X	H_2 and CO_2	1,3-dihydroxyscetone (DHA), glyceraldehyde (GA)	2022	**Pecoraro et al.** https://doi.org/10.1016/j.jiec.2022.11.010
$Bi_2Ti_2O_7$	glycerol	10mM glycerol (photooxidation tests), 50mM glycerol (PR tests)	Pt	H_2	dihydroxyacetone (DHA) and glyceraldehyd (GAD)	2023	**Musso et al.** https://doi.org/10.1016/j.matlet.2022.133346

8. 2 Calculated values of the GC measurements

As supplementary, ***Table 8-11*** provide a summary of all calculated values of the data obtained from GC measurements and detected in ppm. Calculations were made with ***equation (17)***, as previously stated. Herein, ***Table 8*** illustrates the experimental focus of the respective sample and the values of H_2 and CH_4 in µmol/h. The ***Table 9-11***, display the data from the two upscaled experiments.

*Table **8**: Synopsis of calculated values of all discussed samples.*

Experiment type	Sample name	H_2 [µmol/h]	CH_4 [µmol/h]
Preliminary (C)	1/P25-Pt/He/RT	1,146	0,017
Preliminary (*D*)	1/P25/He/RT	0,0006	0,0009
Preliminary (*G*)	1/P25-Pt/He/70°C	1,421	0,090
Preliminary (*H*)	1/P25/He/70°C	0,029*	0,014*
blank	1/P25-Pt/He/RT/D	0	0
blank	1/P25-Pt/He/RT/NC	0,0001	$9{,}97 * 10^{-5}$
blank	P25-Pt/He/RT/NM	0,499*	0,003*
24h (*H*)	1/P25/He/70°C/24h	0,029	0,0007
PET (source 2) (*C*)	2/P25-Pt/He/RT	0,853	0,015
LDPE (*C*)	3/P25-Pt/He/RT	0,382	0,002
PP (*C*)	4/P25-Pt/He/RT	0,454	0,003
solar simulation (*C*)	1/P25-Pt/He/RT/SS	0,119	0,005
solar simulation (H)	1/P25/He/70°C/SS	0,0005	0,001

* calculated mean average from a set of 3 samples

***Table 9**: Obtained mean averages of upscaled experiments, for both H_2 and CH_4 generation.*

Experiment type	Sample name	Hour	H_2 [µmol/h]	CH_4 [µmol/h]
Upscaled (C)	1/P25-Pt/He/RT/UP	0-5	11,64	0,161
		24-32	10,35	0,174
Upscaled (H)	1/P25/He/70°C/UP	0-5	0,063	0,074
		24-32	0,024	0,031

***Table 10**: Overview of all measured samples of 1/P25-Pt/He/RT/UP given in µmol and µmol/h.*

Hour	H_2 [µmol]	H_2 [µmol/h]	CH_4 [µmol]	CH_4 [µmol/h]
0	0	0	0,008	0,008
1	19,57	19,57	0,203	0,203
2	25,62	12,81	0,350	0,175
3	39,60	13,20	0,593	0,198
4	47,37	11,84	0,735	0,184
5	62,13	12,43	0,995	0,199
24	260,48	10,85	4,31	0,180
26	276,54	10,64	4,64	0,178
28	278,79	9,96	4,69	0,167
30	306,15	10,20	5,16	0,172
32	323,11	10,10	5,56	0,174

Table 11: Overview of all measured samples of 1/P25/He/70°C/UP given in µmol and µmol/h.

Hour	H_2 [µmol]	H_2 [µmol/h]	CH_4 [µmol]	CH_4 [µmol/h]
0	0	0	0,012	0,012
1	0,057	0,057	0,083	0,083
2	0,154	0,077	0,171	0,085
3	0,250	0,083	0,268	0,089
4	0,324	0,081	0,361	0,090
5	0,395	0,079	0,433	0,087
24	0,664	0,028	0,823	0,034
26	0,799	0,031	1,02	0,039
28	0,674	0,024	0,870	0,031
30	0,560	0,019	0,734	0,024
32	0,584	0,018	0,816	0,026

8.3 Additional data of the gravimetry

The presented table, ***Table 12***, depicts the weighed sample masses after irradiation and the corresponding total mass loss. Additionally, the sequence in degradation degree, from highest to lowest value, is also visible.

***Table 12**: Gravimetric analysis of preliminary experiments conducted with PET.*

Sample	Mass remaining after irradiation [mg]	Total mass loss [mg]	Degradation degree (from highest to lowest)
1/P25-Pt/CA/RT	8,7	9,3	3
1/P25/CA/RT	15,2	2,8	6
1/P25/He/RT	15,7	2,3	7
1/P25-Pt/CA/70°C	8,9	9,1	4
1/P25/CA/70°C	13,4	4,6	5
1/P25-Pt/He/70°C	5,2	12,8	2
1/P25/He/70°C	4,7	13,3	1

8. 4 Images of filtered solutions

The images, ***Figure 35-39***, shown in this subsection, were taken after filtration of the respective substrate solution. In ***Figure 36*** and ***37***, the pale-yellow colour of *1/P25-Pt/He/70°C* is depicted in contrast to the other obtained samples. The solutions from the two solar simulated and upscaled experiments are illustrated in ***Figure 38*** and ***39***. From comparison of ***Figure 36-39***, it can be derived, that yellow coloration of *1/P25-Pt/He/RT/UP* is more intense than for *1/P25-Pt/He/RT/70°C*.

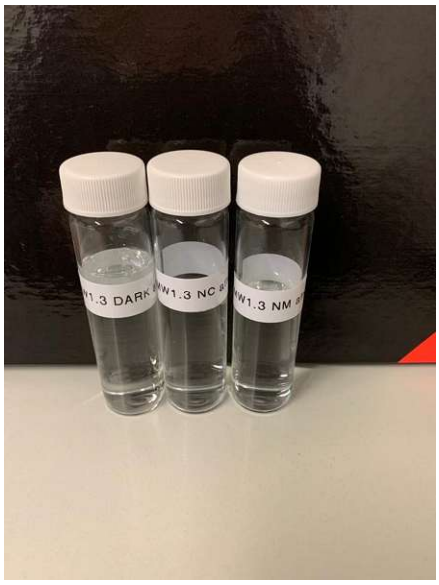

Figure 35*: Sample solutions from blank experiments, after UV irradiation and subsequent filtration, all clear in colour; respective samples (from left to right): 1/P25-Pt/He/RT/D, 1/P25-Pt/He/RT/NC, P25-Pt/He/RT/NM.*

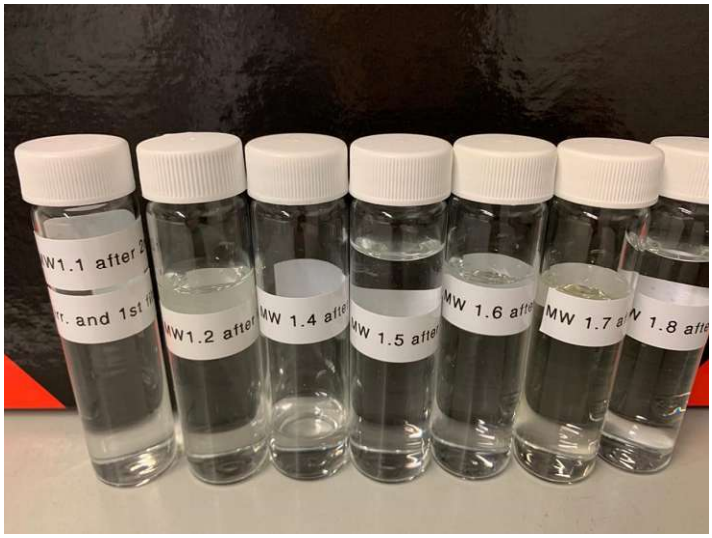

Figure 36*: Sample solutions from preliminary experiments, after UV irradiation and subsequent filtration; respective samples (from left to right): 1/P25-Pt/CA/RT, 1/P25/CA/RT, 1/P25/He/RT, 1/P25-Pt/CA/70°C, 1/P25-Pt/CA/70°C, 1/P25-Pt/He/70°C and 1/P25/He/70°C.*

***Figure 37**: Comparison of sample solution colours; 1/P25-Pt/He/70°C (left) a pale yellow and 1/P25/He/70°C (right) is transparent.*

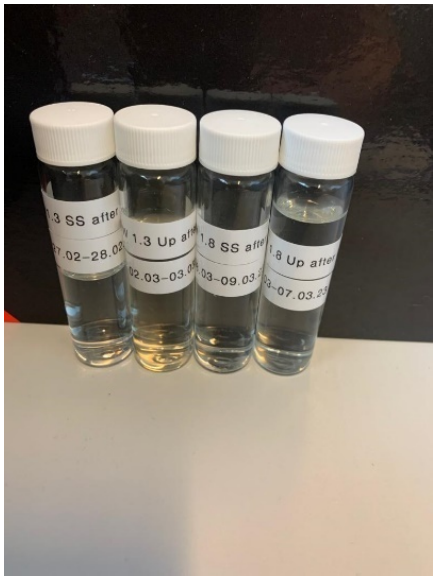

***Figure 38**: Sample solutions from solar simulated and upscaled experiments; respective samples (from left to right): 1/P25-Pt/He/RT/SS, 1/P25-Pt/He/RT/UP, 1/P25/He/70°C/SS, 1/P25/He/70°C/UP.*

***Figure 39**: Comparison of sample solution colours from upscaled experiments; 1/P25-Pt/He/RT/UP (left) an intense yellow colour and 1/P25/He/70°C/UP colourless.*

8.5 Comprehensive analysis of the HPLC data

The evaluation of data obtained from HPLC measurements are demonstrated in ***Table 13-16***. ***Table 13*** summarizes all obtained peak values, classified in retention time windows, given in minutes. Further, the first four samples shown, were produced with CA, the following six under inert conditions. Peak areas of peaks corresponding to a respective compound, depict the calculated concentrations. In contrast, for peaks which cannot be assigned to one of the investigated compounds, the obtained peak area value is shown.

The attained concentration values for each compound is given in ***Table 14-16***. The calculated values were determined from measured peak area values and respective calibration equations from ***Table 5***.

Table 13: *Summary of all measured peaks of all investigated samples.*

Peaks and retention time windows												
							OA				**AA**	**EG**
Sample	1.591-1.612	1.678-1.733	1.803	3.403-3.445	6.034	6.283-6.459	6.822	8.743-8.808	9.811-9.823	11.151	11.985-11.991	12.964
1/P25-Pt/CA/RT						12931*	0,068 mg/ml	8 116 657	11 306			
1/P25/CA/RT						14 266	0,037 mg/ml	6 571 043	10 929			
1/P25-Pt/CA/70°C						30 173	0,025 mg/ml	4 861 323	10 694		0,057 mg/ml	
1/P25/CA/70°		24 117		2 810		20 753		5 453 112	8 443		0,030 mg/mL	0,028 mg/ml
1/P25-Pt/He/70°C		35 739				73 710		5 670 816	21 087		0,095 mg/ml	0,019 mg/ml
1/P25-Pt/He/RT/UP	66 977			5 827		3 783	0,075 mg/mL	5 809 680	5 739		0,081 mg/ml	
1/P25-Pt/He/RT/SS		21 859		7 327		3 308		5 526 785	5 946		0,022 mg/ml	
1/P25/He/70°C/24h	80 843				140 662			5 435 814	28 095		0,023 mg/ml	0,081 mg/ml
1/P25/He/70°C/UP			12 535			51 597		7 117 502	21 273		0,028 mg/ml	0,026 mg/ml
1/P25/He/70°C/SS						37 655		5 709 385	9 730	2 786		0,158 mg/ml

* two peak areas combined

Table 14: *Synopsis of obtained values of OA for respective samples, given in mg/mL.*

Sample	Concentration [mg/mL]
1/P25-Pt/CA/RT	0,068
1/P25/CA/RT	0,037
1/P25-Pt/CA/70°C	0,025
1/P25-Pt/He/RT/UP	0,075

Table 15: *Synopsis of obtained values of AA for respective samples, given in mg/mL.*

Sample	Concentration [mg/mL]
1/P25-Pt/CA/70°C	0,057
1/P25/CA/70°	0,030
1/P25-Pt/He/70°C	0,095
1/P25-Pt/He/RT/UP	0,081
1/P25-Pt/He/RT/SS	0,022
1/P25/He/70°C/24h	0,023
1/P25/He/70°C/UP	0,028

Table 16: *Synopsis of obtained values of EG for respective samples, given in mg/mL.*

Sample	Concentration [mg/mL]
1/P25/CA/70°	0,028
1/P25-Pt/He/70°C	0,019
1/P25/He/70°C/24h	0,081
1/P25/He/70°C/UP	0,026
1/P25/He/70°C/SS	0,158

9. References

1. Wu, G., Li, J. & Xu, Z. Triboelectrostatic separation for granular plastic waste recycling: A review. *Waste Management* **33**, 585–597 (2013).
2. Siddique, R., Khatib, J. & Kaur, I. Use of recycled plastic in concrete: A review. *Waste Management* **28**, 1835–1852 (2008).
3. Narancic, T. & O'Connor, K. E. Plastic waste as a global challenge: Are biodegradable plastics the answer to the plastic waste problem? *Microbiology (United Kingdom)* **165**, 129–137 (2019).
4. Chu, S. *et al.* Photocatalytic Conversion of Plastic Waste: From Photodegradation to Photosynthesis. *Adv Energy Mater* **12**, (2022).
5. Rhodes, C. J. Plastic pollution and potential solutions. **101**, 207–260 (2018).
6. Müller, R. J., Kleeberg, I. & Deckwer, W. D. Biodegradation of polyesters containing aromatic constituents. *J Biotechnol* **86**, 87–95 (2001).
7. Okan, M., Aydin, H. M. & Barsbay, M. Current approaches to waste polymer utilization and minimization: a review. *Journal of Chemical Technology and Biotechnology* **94**, 8–21 (2019).
8. Koelmans, A. A. *et al.* Risk assessment of microplastic particles. doi:10.1038/s41578-021-00411-y.
9. Wang, C., Zhao, J. & Xing, B. Environmental source, fate, and toxicity of microplastics. *J Hazard Mater* **407**, (2021).
10. Jaishankar, M., Tseten, T., Anbalagan, N., Mathew, B. B. & Beeregowda, K. N. Toxicity, mechanism and health effects of some heavy metals. *Interdiscip Toxicol* **7**, 60 (2014).
11. Ashton, K., Holmes, L. & Turner, A. Association of metals with plastic production pellets in the marine environment. *Mar Pollut Bull* **60**, 2050–2055 (2010).
12. Martins, F., Felgueiras, C. & Smitková, M. Fossil fuel energy consumption in European countries. *Energy Procedia* **153**, 107–111 (2018).
13. Lelieveld, J. *et al.* Effects of fossil fuel and total anthropogenic emission removal on public health and climate. *Proc Natl Acad Sci U S A* **116**, 7192–7197 (2019).
14. Diaz, J. H. The influence of global warming on natural disasters and their public health outcomes. *Am J Disaster Med* **2**, 33–42 (2007).
15. Welsby, D., Price, J., Pye, S. & Ekins, P. Unextractable fossil fuels in a 1.5 °C world. *Nature 2021 597:7875* **597**, 230–234 (2021).
16. Wolf, S., Teitge, J., Mielke, J., Schütze, F. & Jaeger, C. The European Green Deal — More Than Climate Neutrality. *Intereconomics 2021 56:2* **56**, 99–107 (2021).
17. Nielsen, T. D., Hasselbalch, J., Holmberg, K. & Stripple, J. Politics and the plastic crisis: A review throughout the plastic life cycle. *Wiley Interdiscip Rev Energy Environ* **9**, e360 (2020).
18. Saeedmanesh, A., Kinnon, M. A. mac & Brouwer, J. Hydrogen is essential for sustainability This review comes from a themed issue on Fuel Cells and Electrolyzers. *Curr Opin Electrochem* **12**, 166–181 (2018).
19. Peksen, M. Hydrogen Technology towards the Solution of Environment-Friendly New Energy Vehicles. *Energies 2021, Vol. 14, Page 4892* **14**, 4892 (2021).
20. Ameta, R., Solanki, M. S., Benjamin, S. & Ameta, S. C. Photocatalysis. *Advanced Oxidation Processes for Wastewater Treatment: Emerging Green Chemical Technology* 135–175 (2018) doi:10.1016/B978-0-12-810499-6.00006-1.
21. Ni, M., Leung, M. K. H., Leung, D. Y. C. & Sumathy, K. A review and recent developments in photocatalytic water-splitting using TiO2 for hydrogen production. *Renewable and Sustainable Energy Reviews* **11**, 401–425 (2007).
22. Ahmed, S. N. & Haider, W. Heterogeneous photocatalysis and its potential applications in water and wastewater treatment: a review. *Nanotechnology* **29**, (2018).

23. Fujishima, A. & Honda, K. Electrochemical Photolysis of Water at a Semiconductor Electrode. *Nature 1972 238:5358* **238**, 37–38 (1972).
24. Fox, M. A. & Dulay, M. T. Heterogeneous Photocatalysis. *Chem Rev* **93**, 341–357 (1993).
25. Qu, Y. & Duan, X. Progress, challenge and perspective of heterogeneous photocatalysts. *Chem Soc Rev* **42**, 2568–2580 (2013).
26. Luttrell, T. *et al.* Why is anatase a better photocatalyst than rutile? - Model studies on epitaxial TiO2 films. *Scientific Reports 2014 4:1* **4**, 1–8 (2014).
27. Kudo, A. & Miseki, Y. Heterogeneous photocatalyst materials for water splitting. *Chem Soc Rev* **38**, 253–278 (2008).
28. Scanlon, D. O. *et al.* Band alignment of rutile and anatase TiO2. *Nature Materials 2013 12:9* **12**, 798–801 (2013).
29. Cheng, L., Xiang, Q., Liao, Y. & Zhang, H. CdS-Based photocatalysts. *Energy Environ Sci* **11**, 1362–1391 (2018).
30. Han, M., Zhu, S., Xia, C. & Yang, B. Photocatalytic upcycling of poly(ethylene terephthalate) plastic to high-value chemicals. (2022) doi:10.1016/j.apcatb.2022.121662.
31. You, J., Guo, Y., Guo, R. & Liu, X. A review of visible light-active photocatalysts for water disinfection: Features and prospects. (2019) doi:10.1016/j.cej.2019.05.071.
32. Moharir, R. v. & Kumar, S. Challenges associated with plastic waste disposal and allied microbial routes for its effective degradation: A comprehensive review. *J Clean Prod* **208**, 65–76 (2019).
33. Sullivan, K. P. *et al.* Mixed plastics waste valorization through tandem chemical oxidation and biological funneling. *Science (1979)* **378**, 207–211 (2022).
34. Zhang, F. *et al.* Current technologies for plastic waste treatment: A review. *J Clean Prod* **282**, (2021).
35. Hu, K. *et al.* Microplastics remediation in aqueous systems: Strategies and technologies. *Water Res* **198**, (2021).
36. Ali, S. S. *et al.* Photocatalytic degradation of low density polyethylene (LDPE) films using titania nanotubes. *Environ Nanotechnol Monit Manag* **5**, 44–53 (2016).
37. Thomas, R. T. & Sandhyarani, N. Enhancement in the photocatalytic degradation of low density polyethylene–TiO2 nanocomposite films under solar irradiation. *RSC Adv* **3**, 14080–14087 (2013).
38. Li, S. *et al.* Polymer-Plastics Technology and Engineering Photocatalytic Degradation of Polyethylene Plastic with Polypyrrole/TiO 2 Nanocomposite as Photocatalyst Photocatalytic Degradation of Polyethylene Plastic with Polypyrrole/TiO 2 Nanocomposite as Photocatalyst. (2010) doi:10.1080/03602550903532166.
39. Uekert, T., Pichler, C. M., Schubert, T. & Reisner, E. Solar-driven reforming of solid waste for a sustainable future. *Nature Sustainability* vol. 4 383–391 Preprint at https://doi.org/10.1038/s41893-020-00650-x (2021).
40. Kawai, T. & Sakata, T. Conversion of carbohydrate into hydrogen fuel by a photocatalytic process. *Nature 286* 474–476 (1980).
41. Kawai, T. & Sakata, T. PHOTOCATALYTIC HYDROGEN PRODUCTION FROM WATER BY THE DECOMPOSITION OF POLY-VINYLCHLORIDE, PROTEIN, ALGAE, DEAD INSECTS, AND EXCREMENT. *Chem Lett* **10**, 81–84 (1981).
42. Linley, S. & Reisner, E. Floating Carbon Nitride Composites for Practical Solar Reforming of Pre-Treated Wastes to Hydrogen Gas. (2023) doi:10.1002/advs.202207314.
43. Wakerley, D. W. *et al.* Solar-driven reforming of lignocellulose to H 2 with a CdS/CdO x photocatalyst. 17021 (2017) doi:10.1038/nenergy.2017.21.
44. Uekert, T., Kuehnel, M. F., Wakerley, D. W. & Reisner, E. Plastic waste as a feedstock for solar-driven H2 generation. *Energy Environ Sci* **11**, 2853–2857 (2018).
45. Du, M. *et al.* Trash to Treasure: Photoreforming of Plastic Waste into Commodity Chemicals and Hydrogen over MoS2-Tipped CdS Nanorods. *ACS Catal* **12**, 12823–12832 (2022).

46. Uekert, T., Kasap, H. & Reisner, E. Photoreforming of Nonrecyclable Plastic Waste over a Carbon Nitride/Nickel Phosphide Catalyst. (2019) doi:10.1021/jacs.9b06872.
47. Nagakawa, H. & Nagata, M. Photoreforming of Organic Waste into Hydrogen Using a Thermally Radiative CdO x/CdS/SiC Photocatalyst. *ACS Appl Mater Interfaces* **13**, 47511–47519 (2021).
48. Kasap, H., Achilleos, D. S., Huang, A. & Reisner, E. Photoreforming of Lignocellulose into H 2 Using Nanoengineered Carbon Nitride under Benign Conditions. (2018) doi:10.1021/jacs.8b07853.
49. Lam, E. & Reisner, E. A TiO2-Co(terpyridine)2 Photocatalyst for the Selective Oxidation of Cellulose to Formate Coupled to the Reduction of CO2 to Syngas. *Angewandte Chemie - International Edition* **60**, 23306–23312 (2021).
50. Uekert, T., Bajada, M. A., Schubert, T., Pichler, C. M. & Reisner, E. Scalable Photocatalyst Panels for Photoreforming of Plastic, Biomass and Mixed Waste in Flow. *ChemSusChem* **14**, 4190–4197 (2021).
51. Achilleos, D. S. *et al.* Solar Reforming of Biomass with Homogeneous Carbon Dots. *Angewandte Chemie - International Edition* **59**, 18184–18188 (2020).
52. Edirisooriya, E. M. N. T. *et al.* Photo-reforming and degradation of waste plastics under UV and visible light for H2 production using nanocomposite photocatalysts. *J Environ Chem Eng* **11**, 109580 (2023).
53. Belda-Marco, S., Lillo-Ródenas, M. A. & Román-Martínez, M. C. H 2 production by cellulose photoreforming with TiO 2-Cu photocatalysts bearing different Cu species. *Catal Today* 413–415 (2023) doi:10.1016/j.cattod.2022.11.006.
54. Džermeikait, K. & Antanaitis, unas. Global Warming and Dairy Cattle: How to Control and Reduce Methane Emission. (2022) doi:10.3390/ani12192687.
55. Wittich, K., Krämer, M., Bottke, N., Schunk, S. A. & Reviews, C. Catalytic Dry Reforming of Methane: Insights from Model Systems. *ChemCatChem* **12**, 2130–2147 (2020).
56. Schultz, D. M. & Yoon, T. P. Solar synthesis: Prospects in visible light photocatalysis. *Science (1979)* **343**, (2014).
57. Spangler, G. E. Gas Chromatography: Theory and Definitions, Retention and Thermodynamics, and Selectivity. in *Analytical Separation Science* (eds. Anderson, J. L., Berthod Alain, Pino Estévez, V. & Stalcup, A. M.) 775–777 (Wiley-VCH Verlag GmbH & Co. KGaA., 2015).
58. Lozano-Sánchez, J., Borrás-Linares, I., Sass-Kiss, A. & Segura-Carretero, A. Chromatographic Technique: High-Performance Liquid Chromatography (HPLC). *Modern Techniques for Food Authentication* 459–526 (2018) doi:10.1016/B978-0-12-814264-6.00013-X.
59. Royer, S.-J., Ferró, S., Wilson, S. T. & Karl, D. M. Production of methane and ethylene from plastic in the environment. (2018) doi:10.1371/journal.pone.0200574.
60. Peter Atkins & Julio de Paula. *Atkin's Physical Chemistry*. (Oxford University Press, 2006).
61. Schubert, J. S. *et al.* Immobilization of Co, Mn, Ni and Fe oxide co-catalysts on TiO 2 for photocatalytic water splitting reactions †. (2019) doi:10.1039/c9ta05637h.
62. Schubert, J. S. *et al.* Elucidating the formation and active state of Cu co-catalysts for photocatalytic hydrogen evolution. *J Mater Chem A Mater* **9**, 21958–21971 (2021).
63. Ayala, P. *et al.* Isolation Strategy towards Earth-Abundant Single-Site Co-Catalysts for Photocatalytic Hydrogen Evolution Reaction. (2021) doi:10.3390/catal11040417.

Additional appendix

To honour my father's creativity I have decided that as serious as science is, a little bit of humour is always welcome, as life is short … and so am I. Enjoy!

Chemistry: it's just all a load of rubbish!

Out of rubbish site, out of mind. A world overpacked with plastic.

Waste material artificial, intelligence required

Getting drastic with plastic.

Plastic needn't be so drastic

From trash to cash/ cash from trash/ cashing on trash.